Irradiated shocks in the W28 A2 outflow

Antoine Gusdorf, LERMA/LRA, Paris, France
Maryvonne Gerin, LERMA/LRA, Paris, France
Pierre Lesaffre, LERMA/LRA, Paris, France
Javier Goicoechea, Centro de Astrobiología (CSIC/INTA), Madrid, Spain
Nicolas Flagey, JPL, Pasadena, USA
…and the PRISMAS Team

What is the W28 A2 outflow ?

Also known as “G5.89-00.39”, or the “Harvey & Forveille 1988” outflow

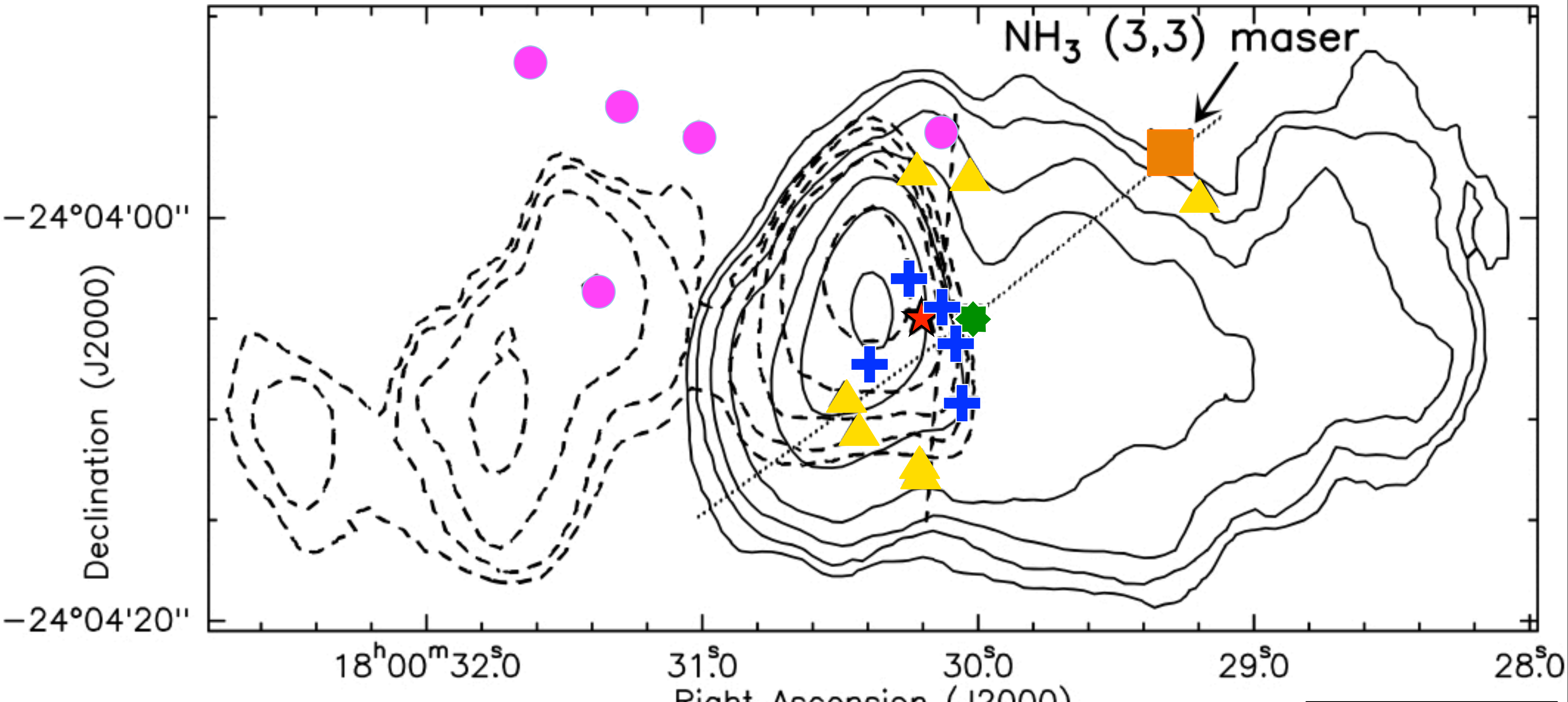

Hunter et al. 2008

- - CO (1-0) 20 to 58 km s^{-1} — CO (1-0) 0 to -37 km s^{-1}

Outline

- MOTIVATIONS
- THE STRUCTURE OF THE W28A2 REGION
- CO OBSERVATIONS
- C I & C^+ OBSERVATIONS
- PERSPECTIVES

MOTIVATIONS

Motivations: ISM & massive star formation

- **The massive star formation problem:**

How to form massive stars despite the radiation pressure ?

  - turbulent core model with a monolithic collapse scenario, scale-up of the low-mass scenario
  - highly dynamical competitive accretion model involving the formation of a cluster

- **The ISM insights:**
  - Physical and chemical processes in a shocked environment
  - The shock is irradiated ; What is its environmental impact ?

Motivations: the energetic balance of galaxies

- CO ladders observations from external galaxies

Large scale effects from PDR, XDR, and shock contributions
NGC 253 Hailey-Dunsheath et al. 2008 ; M82 Panuzzo et al. 2010 ; NGC 891 Nikola et al. 2011 ; NGC 6240 Meijerink et al. 2013

- *Herschel*/PACS observations of NGC1068, Hailey-Dunsheath et al. 2012

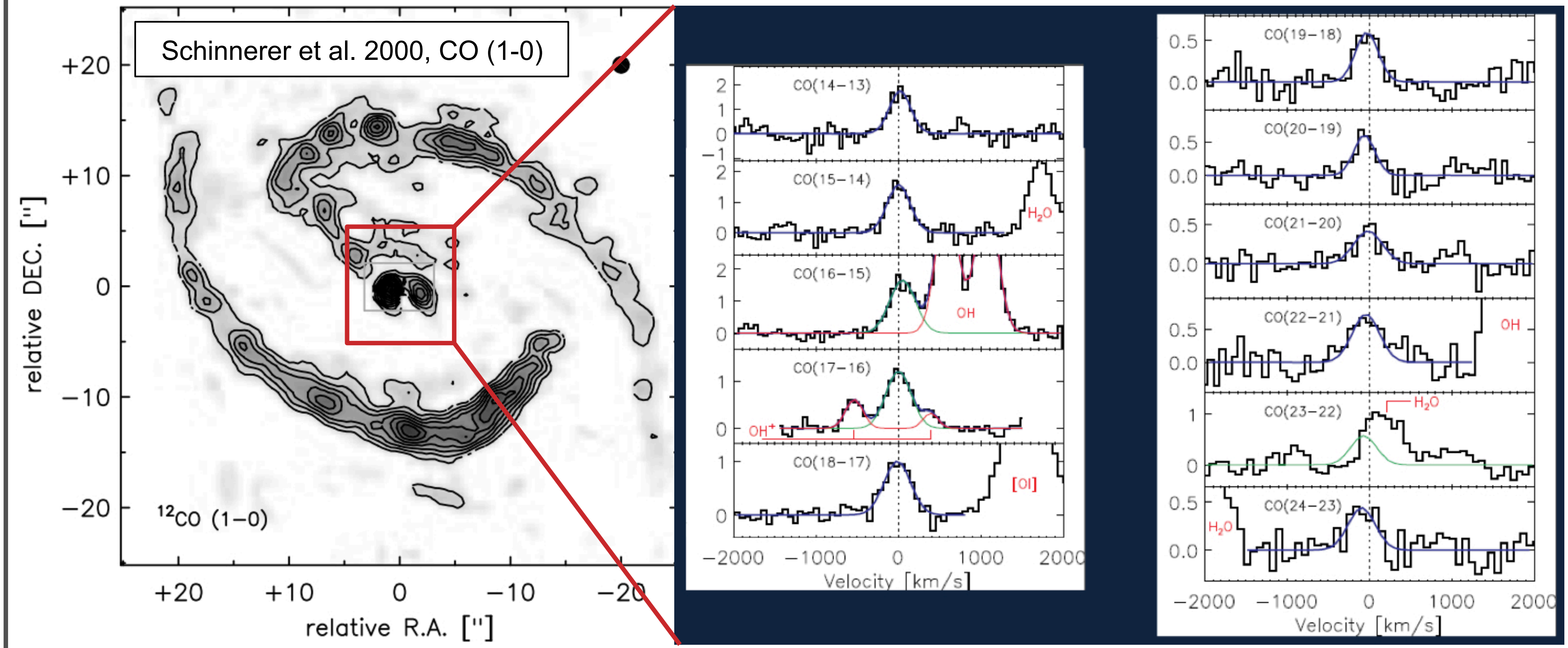

Motivations: the energetic balance of galaxies

Table 4
Heating Mechanisms

	ME	HE	Full
XDR	$n_{\rm H} = 10^{5.75}$ cm^{-3}	$n_{\rm H} = 10^{5.25}$ cm^{-3}	…
	$F_X = 9$ erg cm^{-2} s^{-1}	$F_X = 160$ erg cm^{-2} s^{-1}	…
	$A \sim (130\ \rm pc)^2$	$A \sim (21\ \rm pc)^2$	…
PDR	…	$n_{\rm H} = 10^{6.5}$ cm^{-3}	$n_{\rm H} = 10^{6}$ cm^{-3}
	…	$G_0 = 10^{4.75}$	$G_0 = 10^{5}$
	…	$L_{\rm FUV} \sim 2 \times 10^9\ L_\odot$	$L_{\rm FUV} \sim 10^{10}\ L_\odot$
Shock	C-shock	C-shock	…
	$n_0 = 2 \times 10^5$ cm^{-3}	$n_0 = 10^6$ cm^{-3}	…
	$v = 20$ km s^{-1}	$v = 40$ km s^{-1}	…
	$A \sim (150\ \rm pc)^2$	$A \sim (16\ \rm pc)^2$	…

Notes. Details for the models used in Figure 9. XDR and PDR models are from Meijerink et al. (2007), ME C-shock model is from Flower & Pineau Des Forêts (2010), and HE C-shock model is from Kaufman & Neufeld (1996).

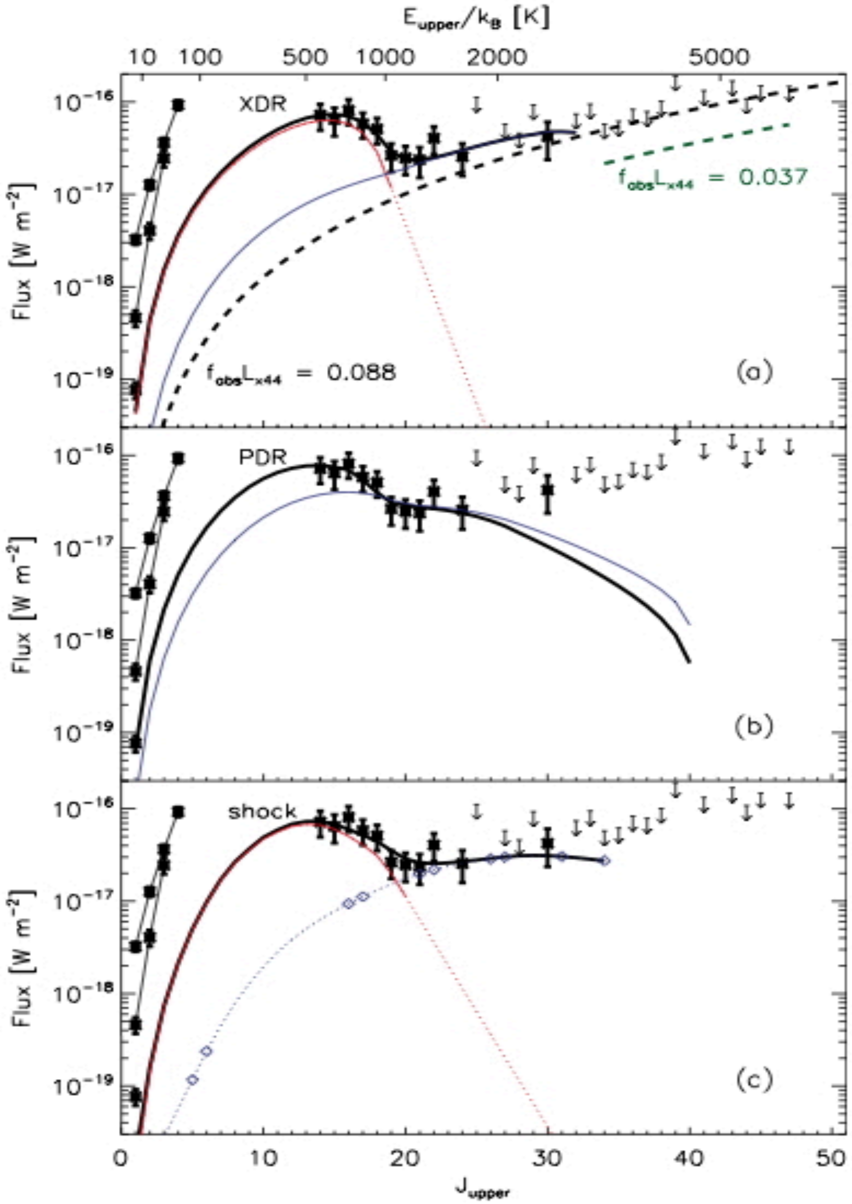

Motivations: the very-high energy point of view

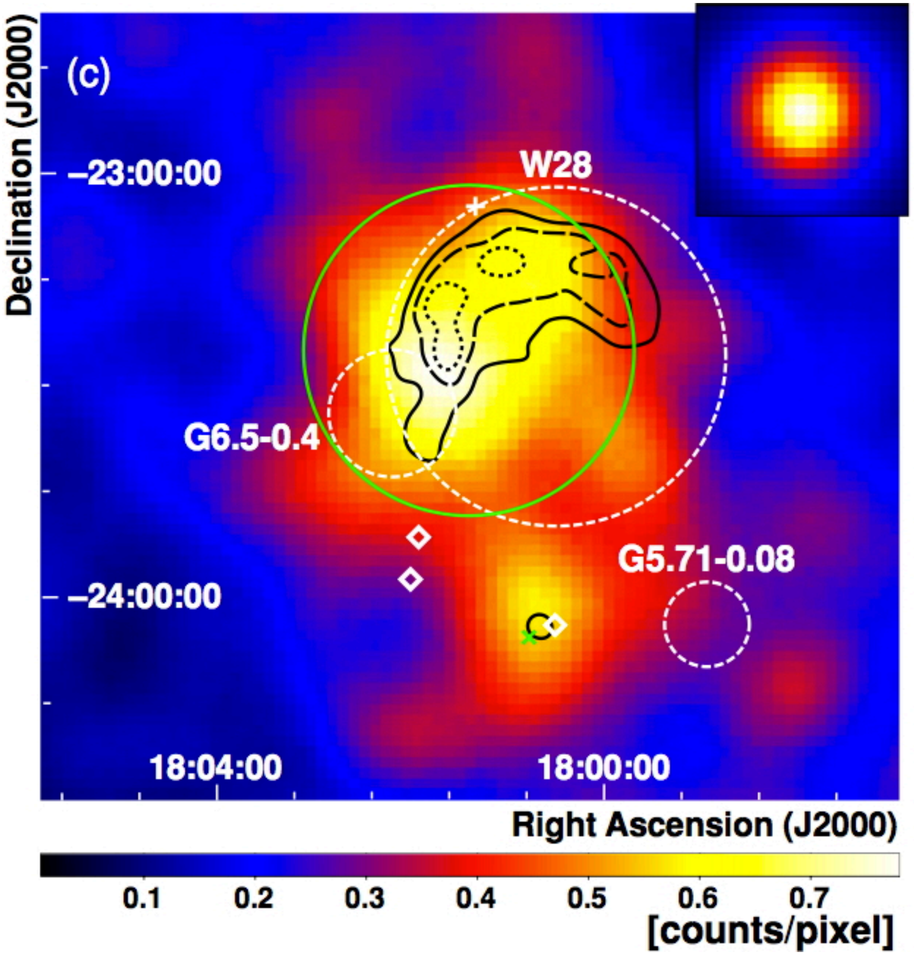

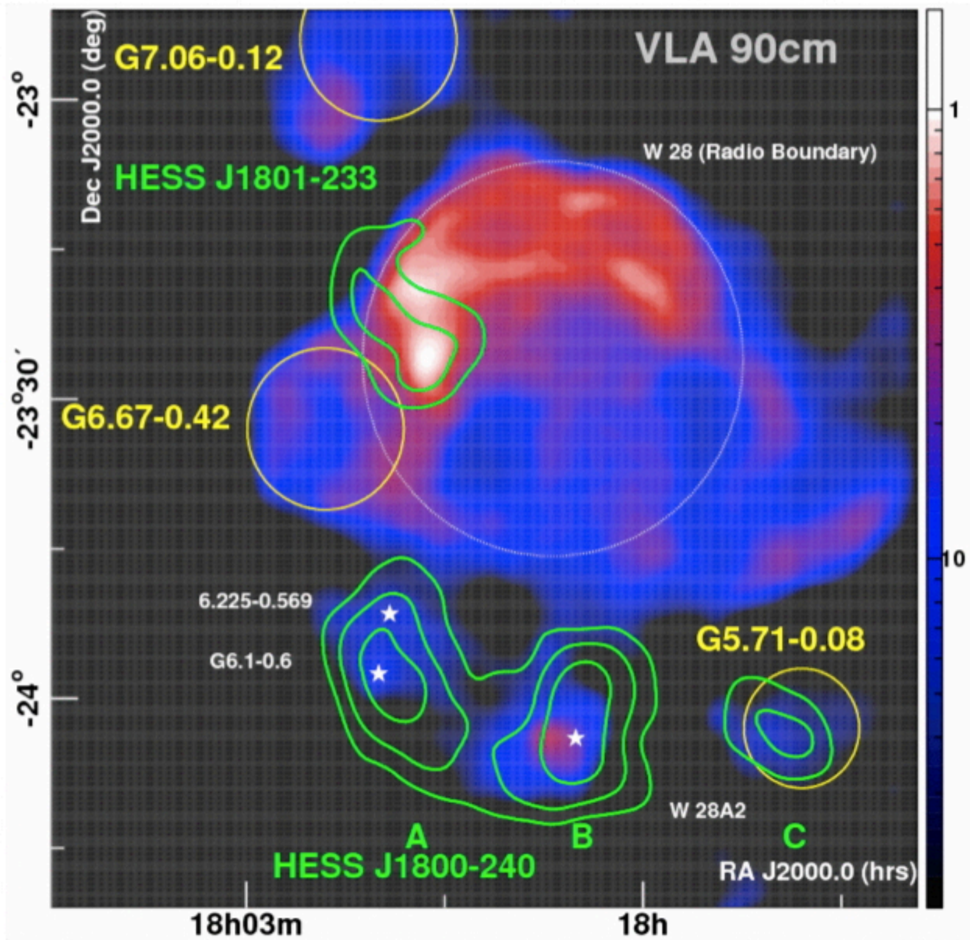

- The Fermi-lat count map

2-10 GeV with 0.2° resolution

Abdo et al. 2010

- The HESS count map

Above 320 GeV with 5-6’ resolution

Aharonian et al. 2008

Motivations: the very-high energy point of view

- Origin of the γ-rays emission: partly due to **cosmic rays**
  - collisions with the ambient gas: hadrons -> π^0 -> detectable γ-rays
  - Inverse Compton effect relativistic e^- - low-E photons
  - Bremsstrahlung of relativistic e^- on electrons of interstellar nuclei
  - Possible neighbouring Pulsar Wind Nebula

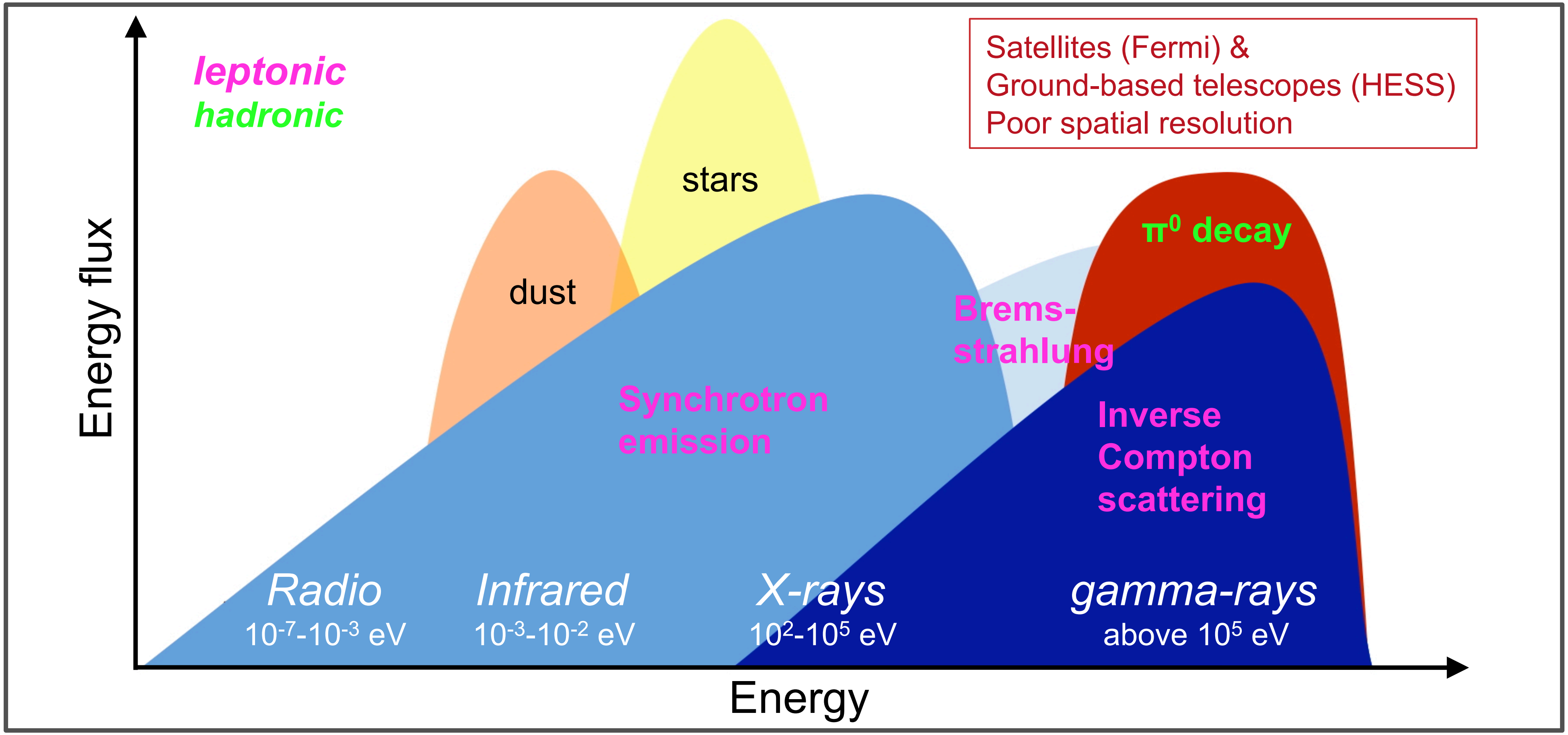

Motivations: the very-high energy point of view

- Origin of the γ-rays emission: partly due to **cosmic rays**
  - collisions with the ambient gas: hadrons -> π^0 -> detectable γ-rays
  - Inverse Compton effect relativistic e^- - low-E photons
  - Bremsstrahlung of relativistic e^- on electrons of interstellar nuclei
  - Possible neighbouring Pulsar Wind Nebula

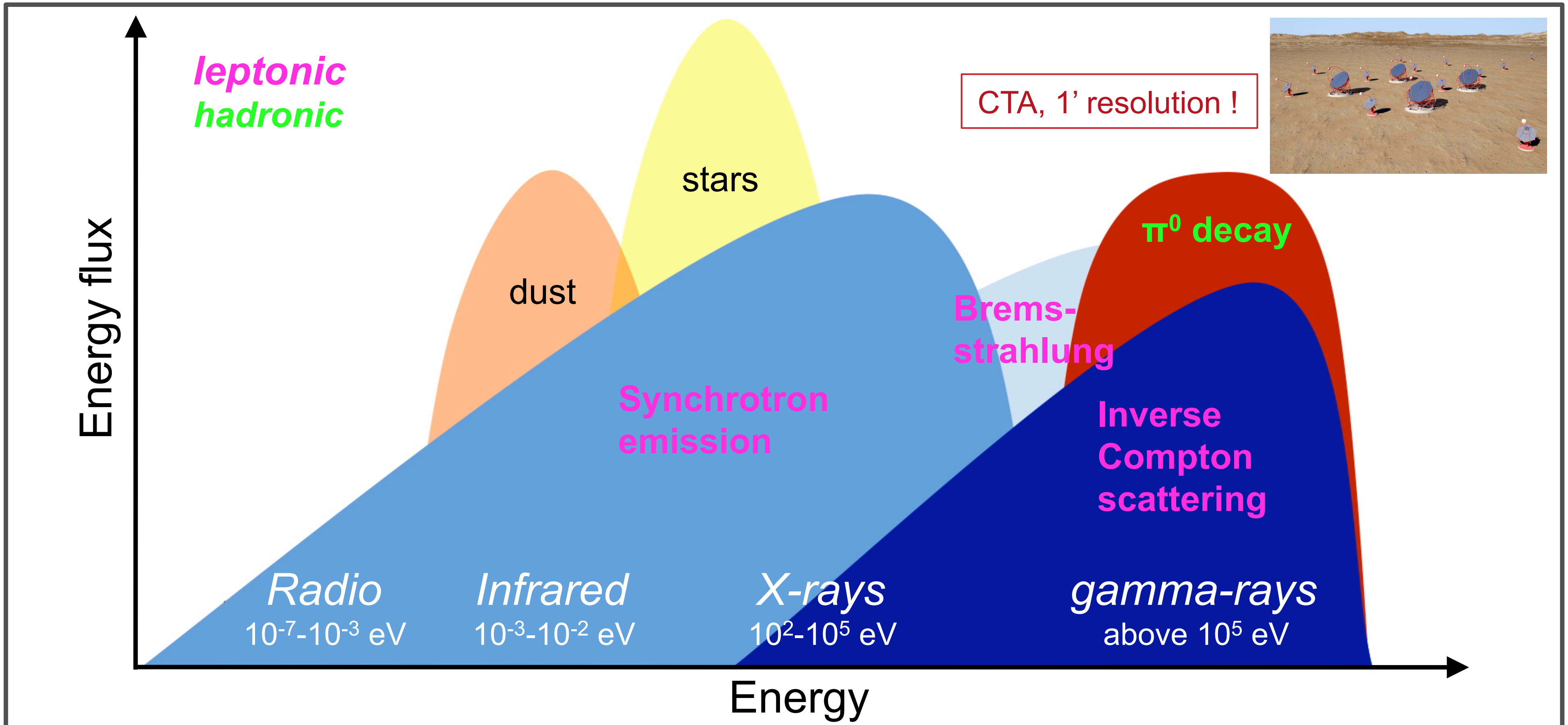

THE STRUCTURE OF THE W28A2 REGION

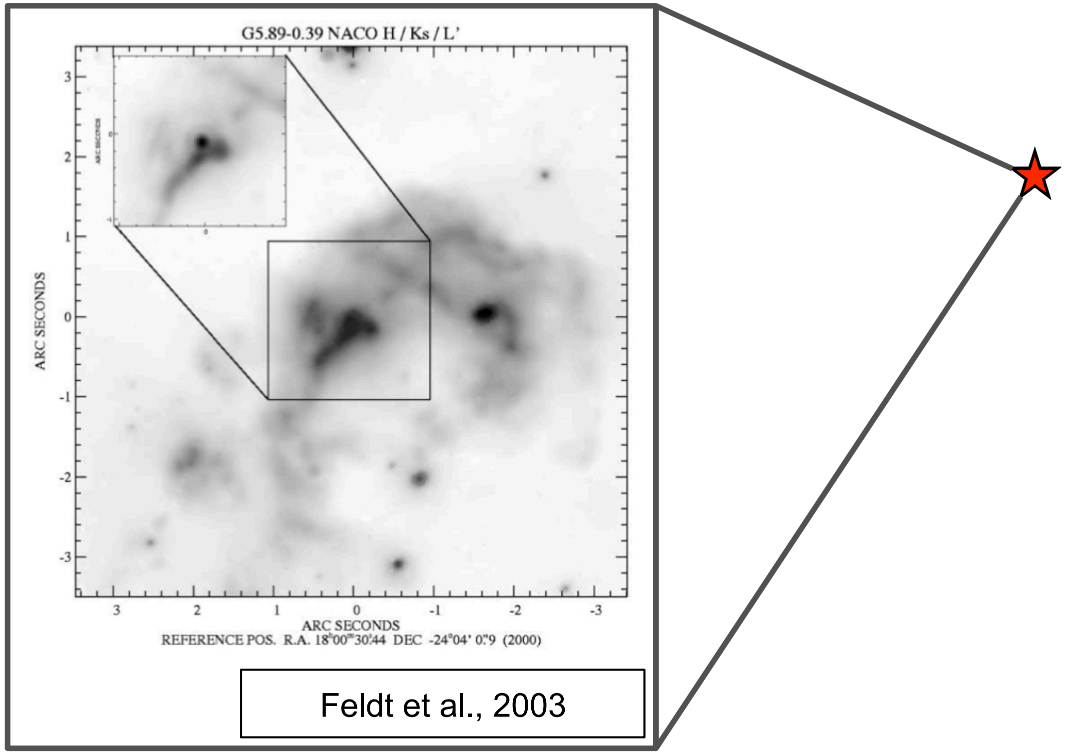

- One central, ionising star: type O3-O8 (Feldt et al. 1999, 2003)

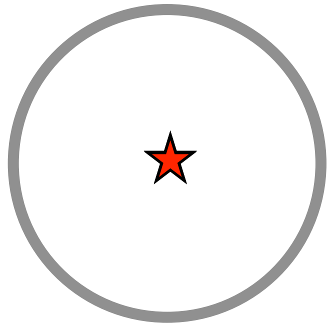

- One central, ionising star: type O3-O8 (Feldt et al. 1999, 2003)
- The beam of our observations, ~12” (Gusdorf et al., in prep)

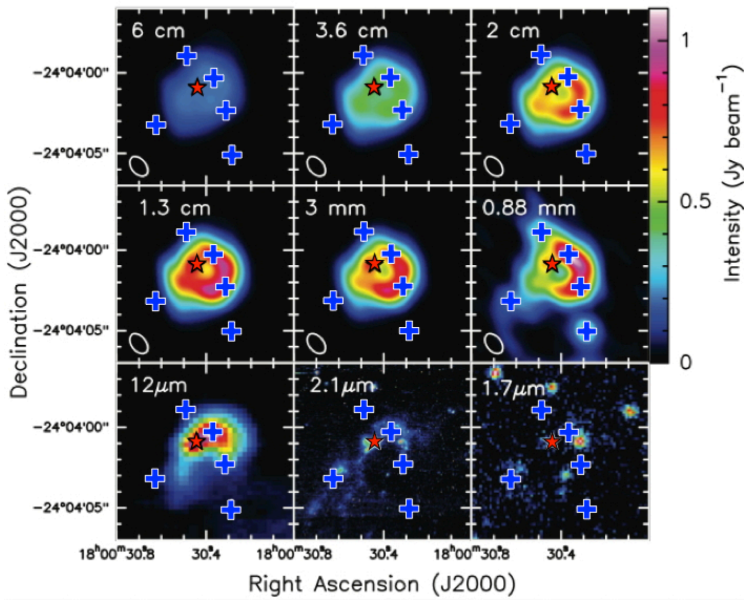

Hunter et al., 2008

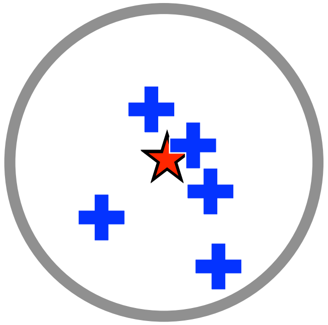

- One central, ionising star: type O3-O8 (Feldt et al. 1999, 2003)
- The beam of our observations, ~12" (Gusdorf et al., in prep)
- Five radio sources (Hunter et al. 2008)

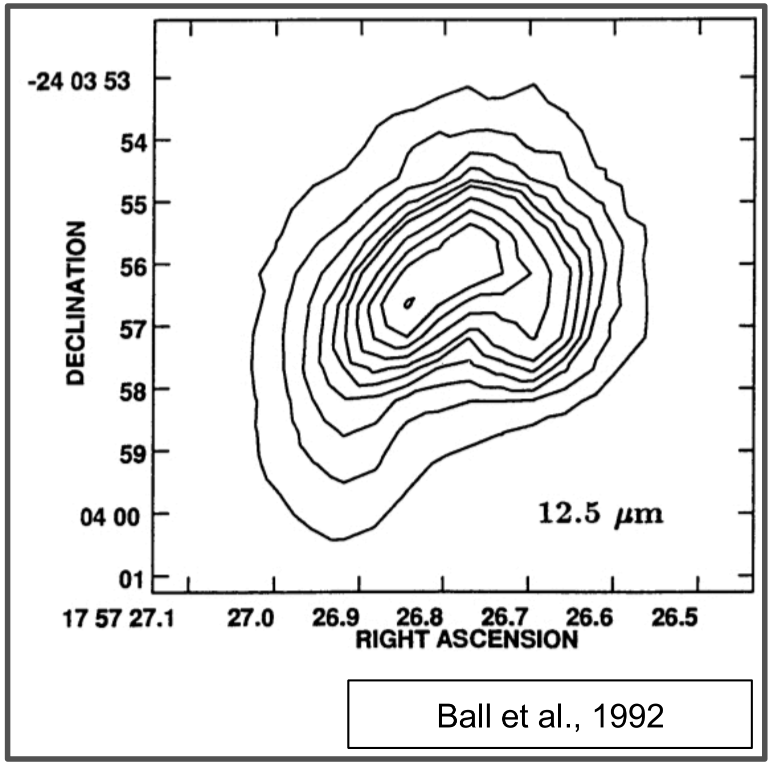

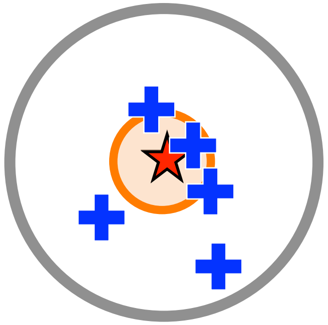

- One central, ionising star: type O3-O8 (Feldt et al. 1999, 2003)
- The beam of our observations, ~12” (Gusdorf et al., in prep)
- Five radio sources (Hunter et al. 2008)
- An ultra compact H II region (Moorwood & Salinari 1983, Lightfoot 1984, Ball et al. 1992) …

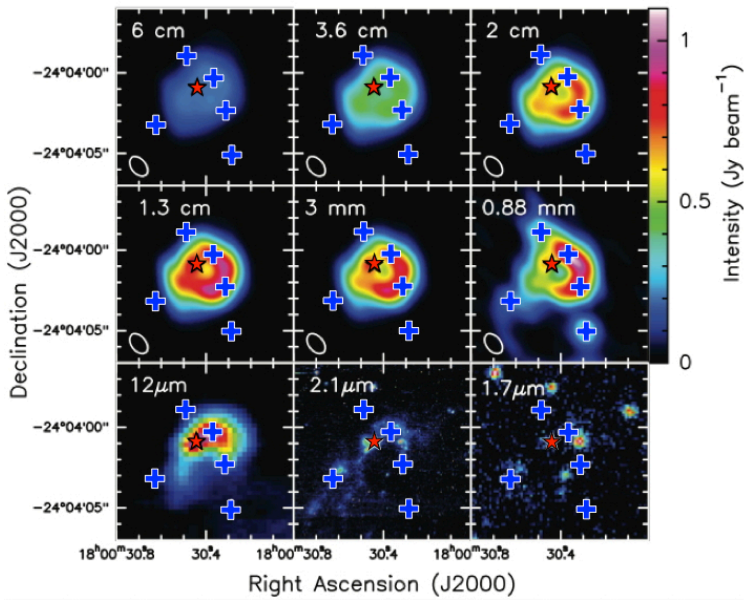

Hunter et al., 2008

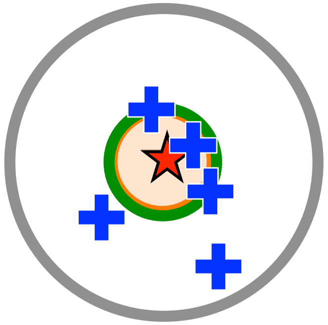

- One central, ionising star: type O3-O8 (Feldt et al. 1999, 2003)
- The beam of our observations, ~12” (Gusdorf et al., in prep)
- Five radio sources (Hunter et al. 2008)
- An ultra compact H II region (Moorwood & Salinari 1983, Lightfoot 1984, Ball et al. 1992) …
- Surrounded by a dusty shell, a PDR in our modelling (Hunter et al. 2008)

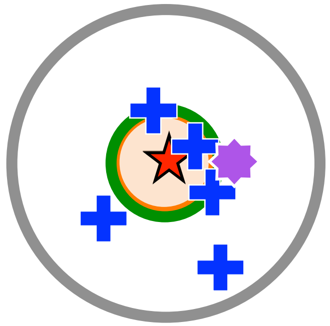

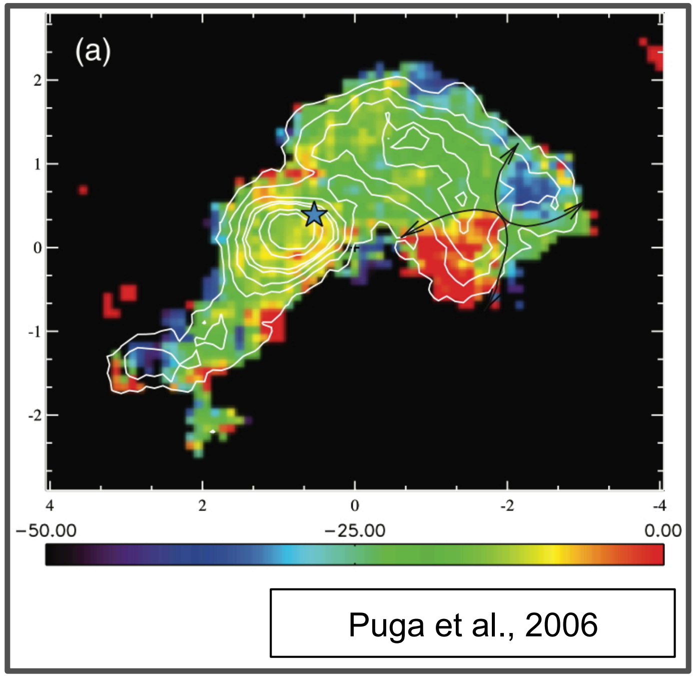

- One central, ionising star: type O3-O8 (Feldt et al. 1999, 2003)
- The beam of our observations, ~12” (Gusdorf et al., in prep)
- Five radio sources (Hunter et al. 2008)
- An ultra compact H II region (Moorwood & Salinari 1983, Lightfoot 1984, Ball et al. 1992) …
- Surrounded by a dusty shell, a PDR in our modelling (Hunter et al. 2008)
- A Brγ bipolar outflow (Puga et al. 2006)

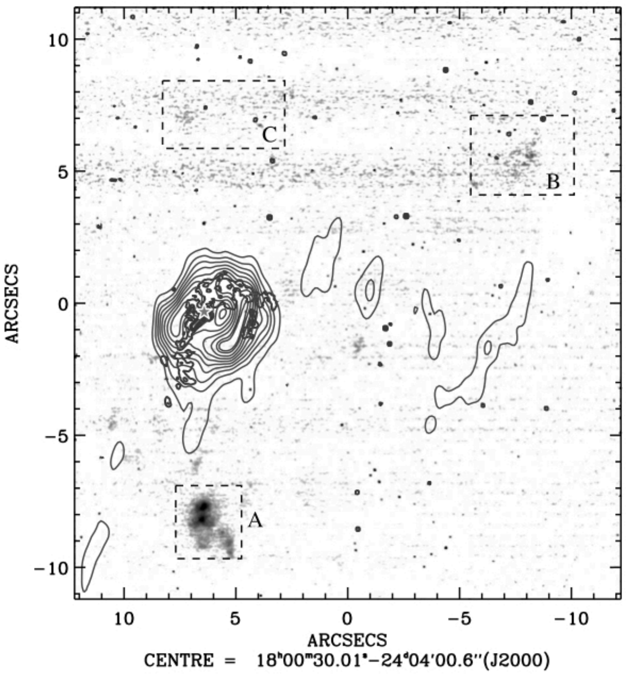

Puga et al., 2006

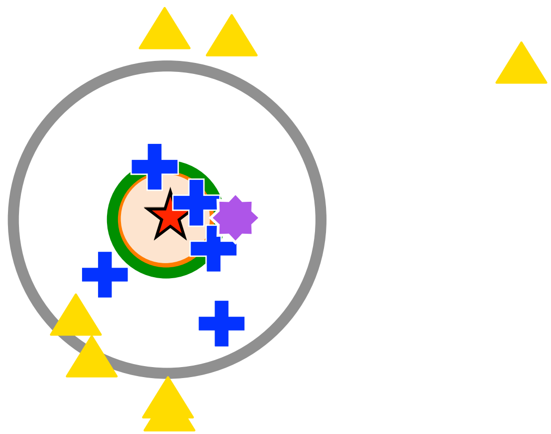

- One central, ionising star: type O3-O8 (Feldt et al. 1999, 2003)
- The beam of our observations, ~12” (Gusdorf et al., in prep)
- Five radio sources (Hunter et al. 2008)
- An ultra compact H II region (Moorwood & Salinari 1983, Lightfoot 1984, Ball et al. 1992) …
- Surrounded by a dusty shell, a PDR in our modelling (Hunter et al. 2008)
- A Brγ bipolar outflow (Puga et al. 2006)
- H_2 knots at 2.12 μm, marking the apex of two outflows (Puga et al. 2006)

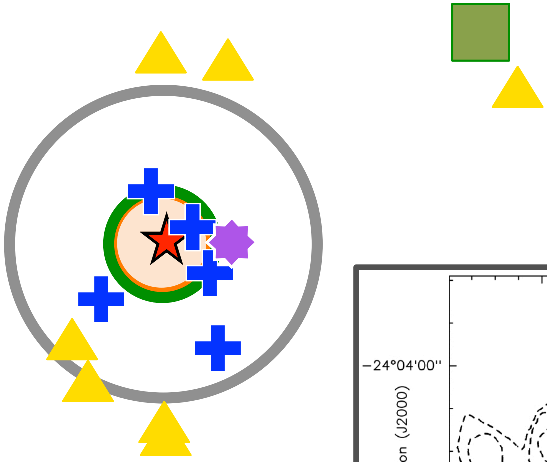

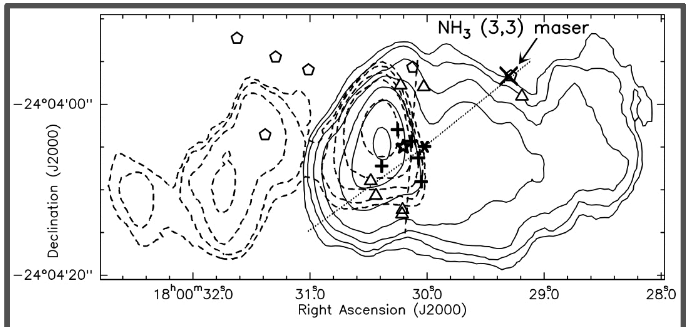

Hunter et al., 2008

- One central, ionising star: type O3-O8 (Feldt et al. 1999, 2003)
- The beam of our observations, ~12" (Gusdorf et al., in prep)
- Five radio sources (Hunter et al. 2008)
- An ultra compact H II region (Moorwood & Salinari 1983, Lightfoot 1984, Ball et al. 1992) …
- Surrounded by a dusty shell, a PDR in our modelling (Hunter et al. 2008)
- A Brγ bipolar outflow (Puga et al. 2006)
- H_2 knots at 2.12 µm, marking the apex of two outflows (Puga et al. 2006)
- One NH_3 maser spot (Hunter et al. 2008)

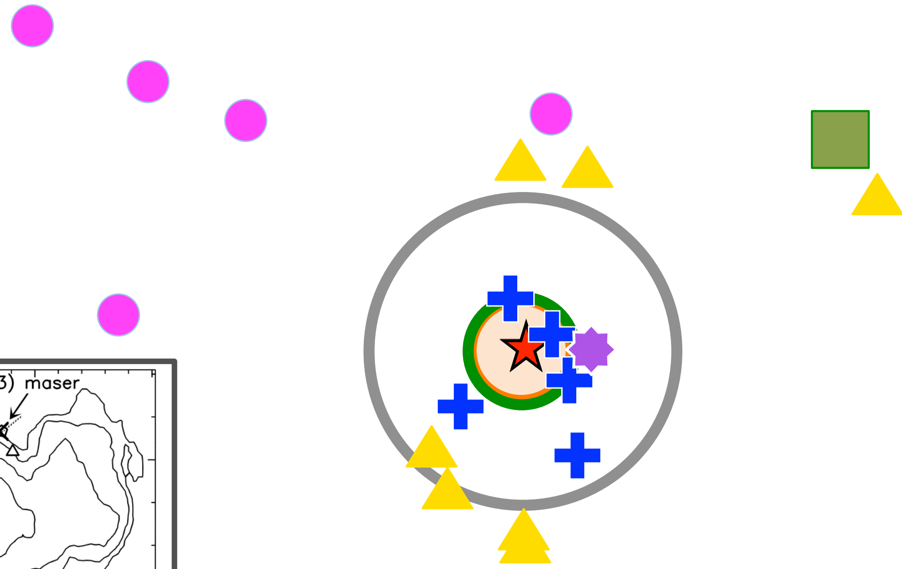

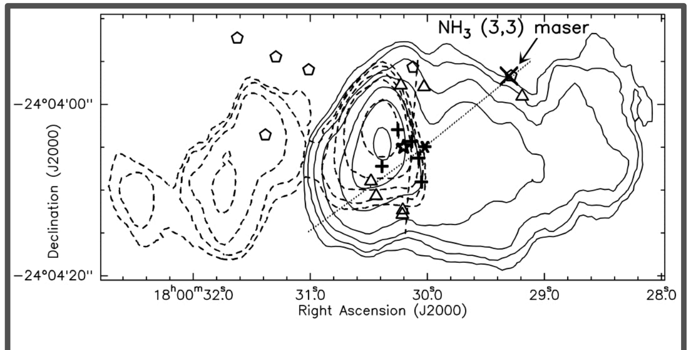

Hunter et al., 2008

- One central, ionising star: type O3-O8 (Feldt et al. 1999, 2003)
- The beam of our observations, ~12” (Gusdorf et al., in prep)
- Five radio sources (Hunter et al. 2008)
- An ultra compact H II region (Moorwood & Salinari 1983, Lightfoot 1984, Ball et al. 1992) …
- Surrounded by a dusty shell, a PDR in our modelling (Hunter et al. 2008)
- A Brγ bipolar outflow (Puga et al. 2006)
- H_2 knots at 2.12 μm, marking the apex of two outflows (Puga et al. 2006)
- One NH_3 maser spot (Hunter et al. 2008)
- Class I CH_3OH maser (Kurtz et al. 2004)

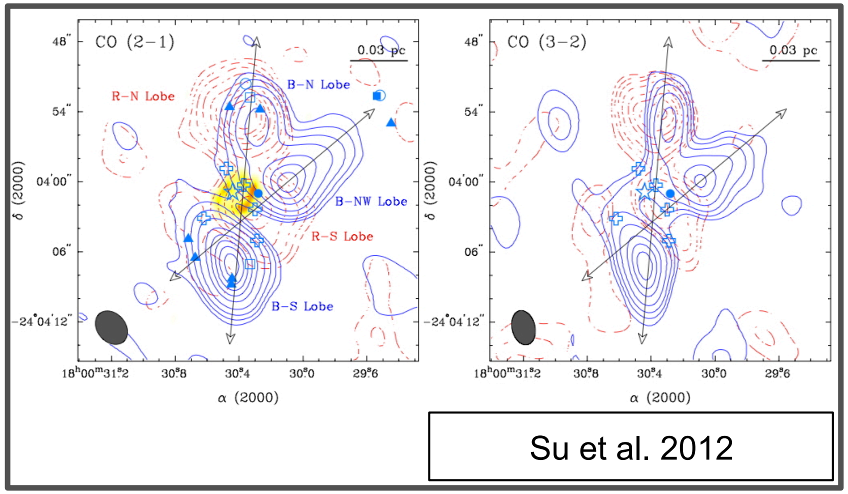

Su et al. 2012

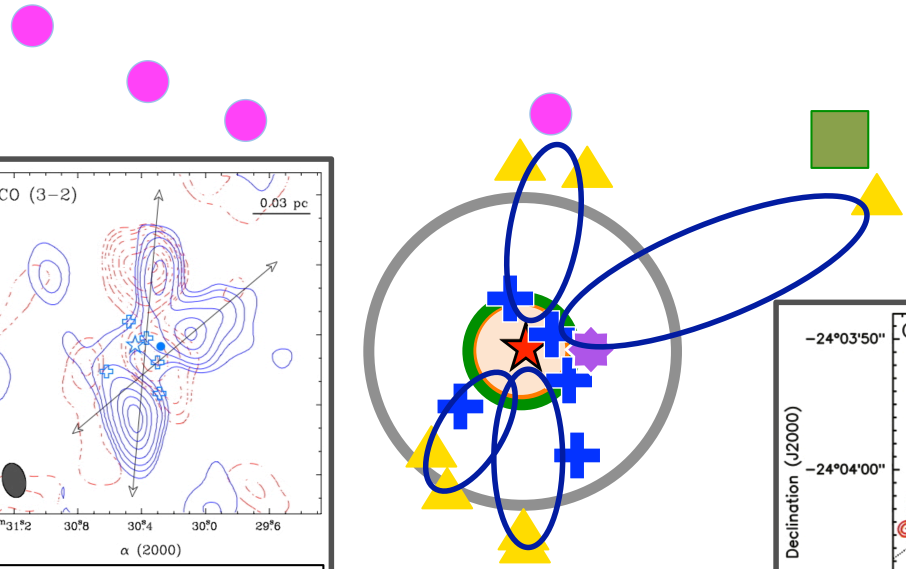

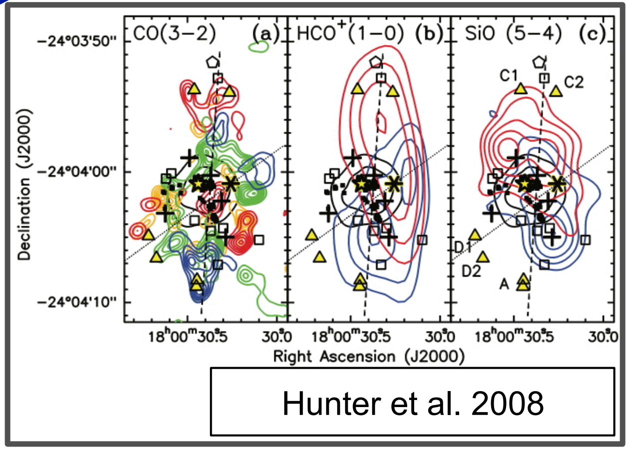

Hunter et al. 2008

- One central, ionising star: type O3-O8 (Feldt et al. 1999, 2003)
- The beam of our observations, ~12” (Gusdorf et al., in prep)
- Five radio sources (Hunter et al. 2008)
- An ultra compact H II region (Moorwood & Salinari 1983, Lightfoot 1984, Ball et al. 1992) …
- Surrounded by a dusty shell, a PDR in our modelling (Hunter et al. 2008)
- A Brγ bipolar outflow (Puga et al. 2006)
- H_2 knots at 2.12 μm, marking the apex of two outflows (Puga et al. 2006)
- One NH_3 maser spot (Hunter et al. 2008)
- Class I CH_3OH maser (Kurtz et al. 2004)
- Two small outflows, seen in SiO (Sollins et al. 2004, Klaassen et al. 2006), CO (Klaassen et al. 2006 Hunter et al. 2008, Su et al. 2012), and other tracers (HCO^+, Klaassen et al. 2006 and Hunter et al. 2008)

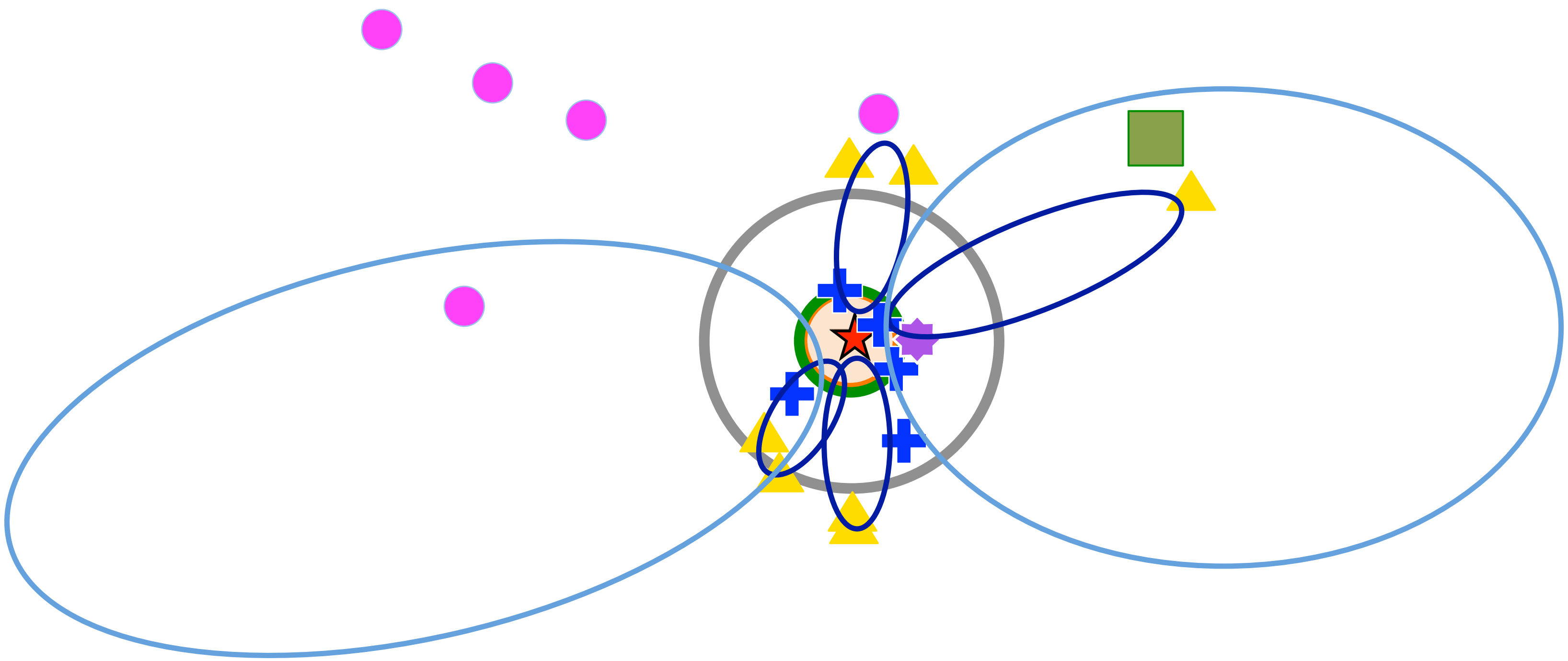

- One central, ionising star: type O3-O8 (Feldt et al. 1999, 2003)
- The beam of our observations, ~12” (Gusdorf et al., in prep)
- Five radio sources (Hunter et al. 2008)
- An ultra compact H II region (Moorwood & Salinari 1983, Lightfoot 1984, Ball et al. 1992) …
- Surrounded by a dusty shell, a PDR in our modelling (Hunter et al. 2008)
- A Brγ bipolar outflow (Puga et al. 2006)
- H_2 knots at 2.12 μm, marking the apex of two outflows (Puga et al. 2006)
- One NH_3 maser spot (Hunter et al. 2008)
- Class I CH_3OH maser (Kurtz et al. 2004)
- Two small outflows, seen in SiO (Sollins et al. 2004, Klaassen et al. 2006), CO (Klaassen et al. 2006 Hunter et al. 2008, Su et al. 2012), and other tracers (HCO^+, Klaassen et al. 2006 and Hunter et al. 2008)
- A massive bipolar outflow seen in CO (Harvey & Forveille 1988)

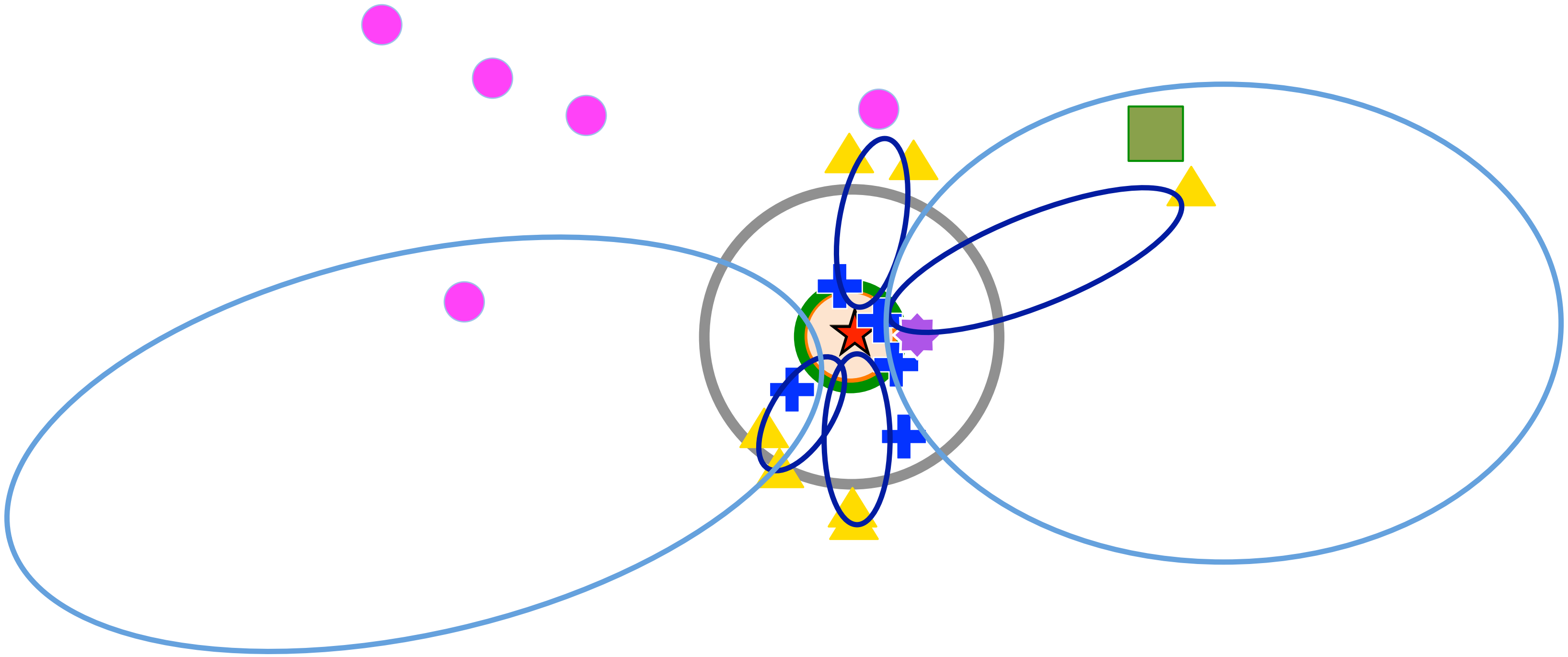

- One central, ionising star: type O3-O8 (Feldt et al. 1999, 2003)
- The beam of our observations, ~12” (Gusdorf et al., in prep)
- Five radio sources (Hunter et al. 2008)
- An ultra compact H II region (Moorwood & Salinari 1983, Lightfoot 1984, Ball et al. 1992) …
- Surrounded by a dusty shell, a PDR in our modelling (Hunter et al. 2008)
- A Brγ bipolar outflow (Puga et al. 2006)
- H_2 knots at 2.12 μm, marking the apex of two outflows (Puga et al. 2006)
- One NH_3 maser spot (Hunter et al. 2008)
- Class I CH_3OH maser (Kurtz et al. 2004)
- Two small outflows, seen in SiO (Sollins et al. 2004, Klaassen et al. 2006), CO (Klaassen et al. 2006 Hunter et al. 2008, Su et al. 2012), and other tracers (HCO^+, Klaassen et al. 2006 and Hunter et al. 2008)
- A massive bipolar outflow seen in CO (Harvey & Forveille 1988)
- Also not shown: H_2O masers (Hofner & Churchwell 1996), and OH masers (Stark et al. 2007)

The wide scale

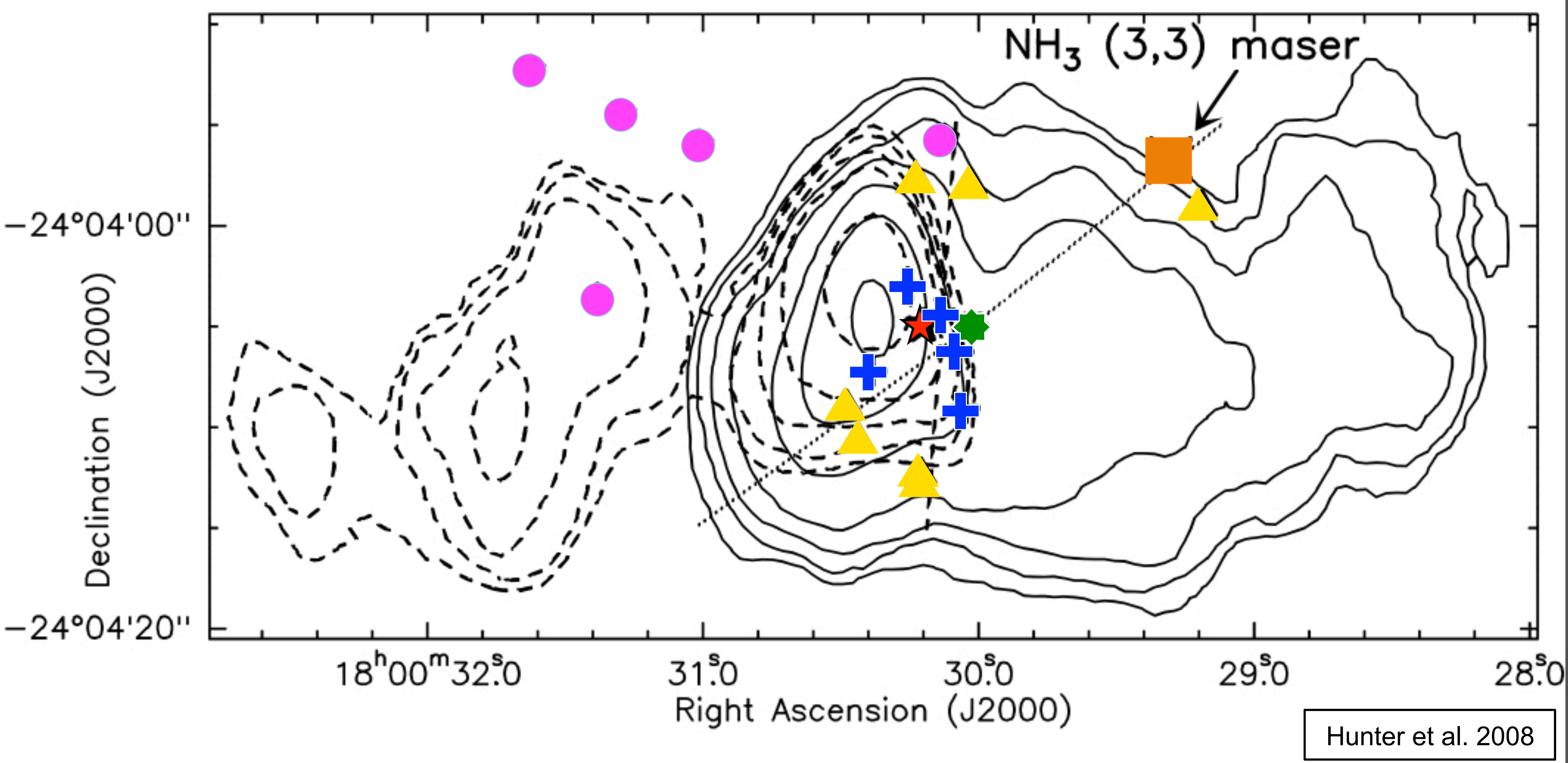

- - CO (1-0) 20 to 58 km s^{-1} — CO (1-0) 0 to -37 km s^{-1}

Other existing constraints

- **Outflows:** 3 bipolar, more or less exposed to protostellar UV field
- **Distance:**
  - Old estimates: 1.9-4 kpc (Velazquez et al. 2002, Fish et al. 2003) ; Hunter et al. 2008 used 2.6 kpc
  - more recently: 1.28 kpc, by Motogi et al. 2011
- **The central star:**
  - Old estimates: O4-O8.5
  - Direct observations by Feldt et al. 2003 : O5
  - Classification by Motogi et al. 2011 : O8
- **Magnetic field:**
  - OH masers : 1.49 mG (Caswell 2001), [-2.4;1.2] mG (Fish & Reid 2006), [-2;2] mG (Stark et al. 2007)
  - Dust continuum polarization studies : 2-3 mG (Tang et al. 2009)

Some conclusions from former studies

ref.	Harvey & Forveille (1988)	Choi et al. (1993)	Acord et al. (1997)	Klaassen et al. (2006)	Watson et al. (2007)
method	CO (1–0), ^{13}CO (1–0)	CO & ^{13}CO (2–1), CO & ^{13}CO (3–2)	SiO (1–0), (2–1) (3–2), (5–4)	CO & ^{13}CO (3–2), SiO (5–4), (8–7)	CO & ^{13}CO (1–0), C^{18}O (1–0)
d (kpc)	3	3	3	2	2
i (°)	0	0	0	45	90
Θ (″)	20	30$^{(1)}$	18	14	7×3
r (pc)	≥ 0.44	≥ 0.15	0.04	0.55	0.32
T (K)	20	10-200$^{(2)}$	$\geq 100^{(3)}$	$\geq 100^{(4)}$	–
n_{H2} (cm^{-3})	$\geq 10^5$	10^4 - 10^6	6.3×10^5	10^6	10^5 - 10^6
M ($M_\odot$)	70$^{(5)}$	0.3$^{(6)}$ -40.4$^{(7)}$	77	3.3	239
P ($M_\odot$ km s^{-1})	1600$^{(8)}$	11.6$^{(6)}$ -593$^{(7)}$	990	96	1703
E (10^{45} ergs)	800$^{(8)}$	4.7$^{(6)}$ -113$^{(7)}$	500	34.6	117
age (yr)	2000	1900	3000	2000	≤ 7700
L ($L_\odot$)	1600	20.3$^{(6)}$ -464$^{(7)}$	1300	141	124
$\dot{M}$ ($M_\odot$ yr^{-1})	0.035	0.0003$^{(6)}$ -0.021$^{(7)}$	0.026	0.0017	0.031
$\dot{P}$ ($M_\odot$ km s^{-1} yr^{-1})	0.8	0.006$^{(6)}$ -0.31$^{(7)}$	0.33	0.0675	0.22

(1) different filling factors are associated to lines with different beam sizes
(2) kinetic temperature based assumption
(3) kinetic temperature based NH_3 (3,3), (4,4), and (5,5) lines
(4) kinetic temperature based on the CO line temperature, SO_2 detection and AWC97
(5) based on ^{13}CO 'inner wings'
(6) assuming that the sources are neutral atomic wind
(7) assuming that the sources are swept-up molecular gas
(8) based on CO extremely high-velocity wings

CO OBSERVATIONS

APEX CO observations: the data

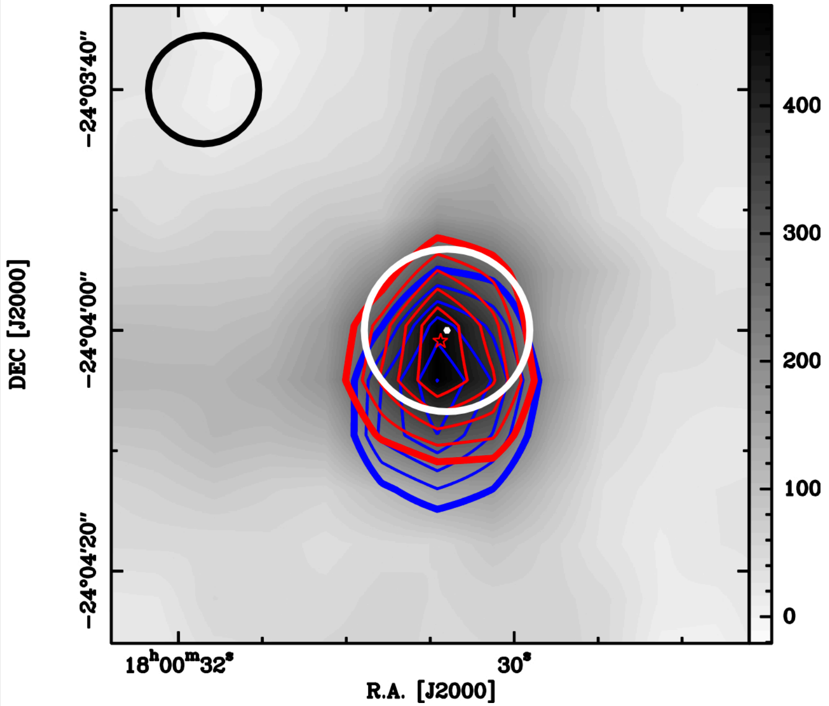

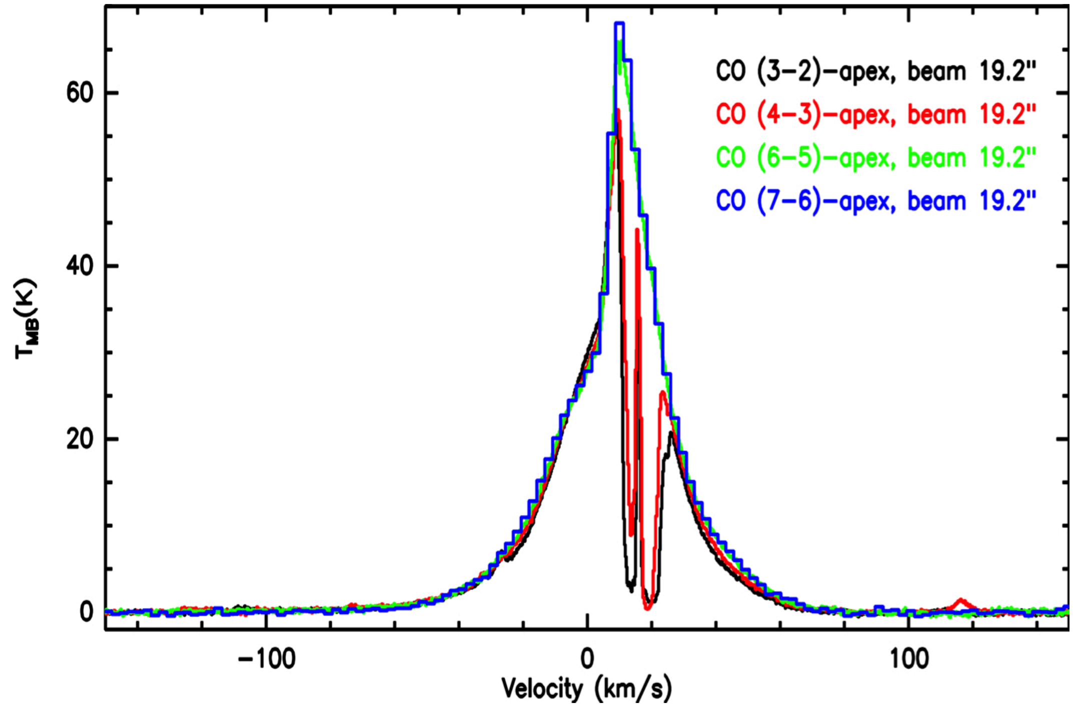

- APEX CO (6-5) line map:
  - total integrated intensity -100 to 100 km/s
  - blue-shifted integrated intensity -100 to 4 km/s
  - red-shifted integrated intensity 16.5 to 100 km/s

- The white beam is the beam of our analysis ~12.5”

=> We consider a filling factor of 1 for CO

APEX CO observations: optical thickness

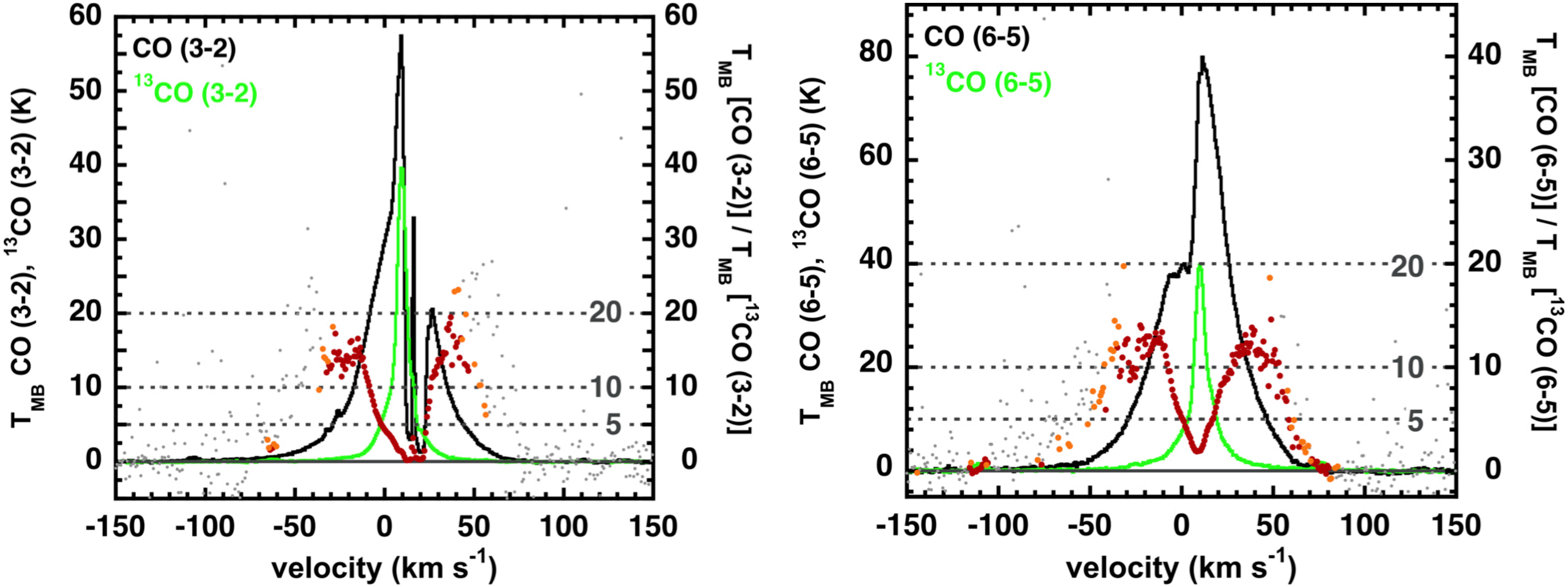

- Red dots: 3σ detection for ^{13}CO

Orange dots: 2σ detection for ^{13}CO

Grey dots: less than 2σ detection for ^{13}CO

Line ratio ~ 5 to 15

=> CO lines accessible from the ground are optically thick, even in the wings

Herschel CO observations

- Two lines are of particular importance:
  - CO (16-15) by HIFI & PACS, single pointing => calibration & gas distribution over the whole velocity range
  - CO (15-14) PACS ^{12,13}CO observations => ratio ~ 47 optically thin !

=> Rotational diagram over a 12.5" area

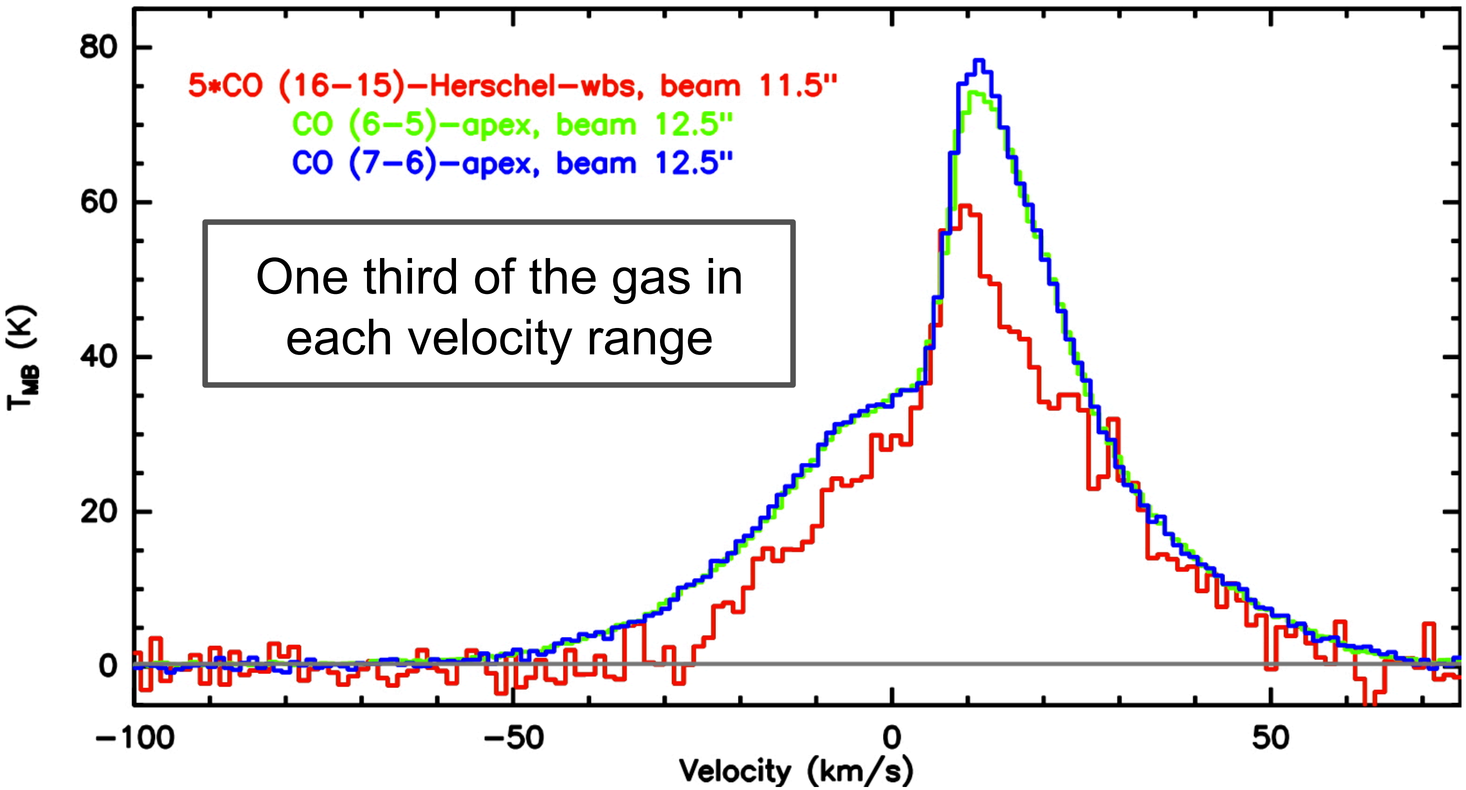

Herschel CO observations

- Summary:
  - APEX => filling factor = 1 for beam of 12.5”, low-*J* are optically thick
  - *Herschel* => higher-*J* lines optically thin, HIFI-PACS cross-calibration
  - Both show a similar gas distribution in the line wings

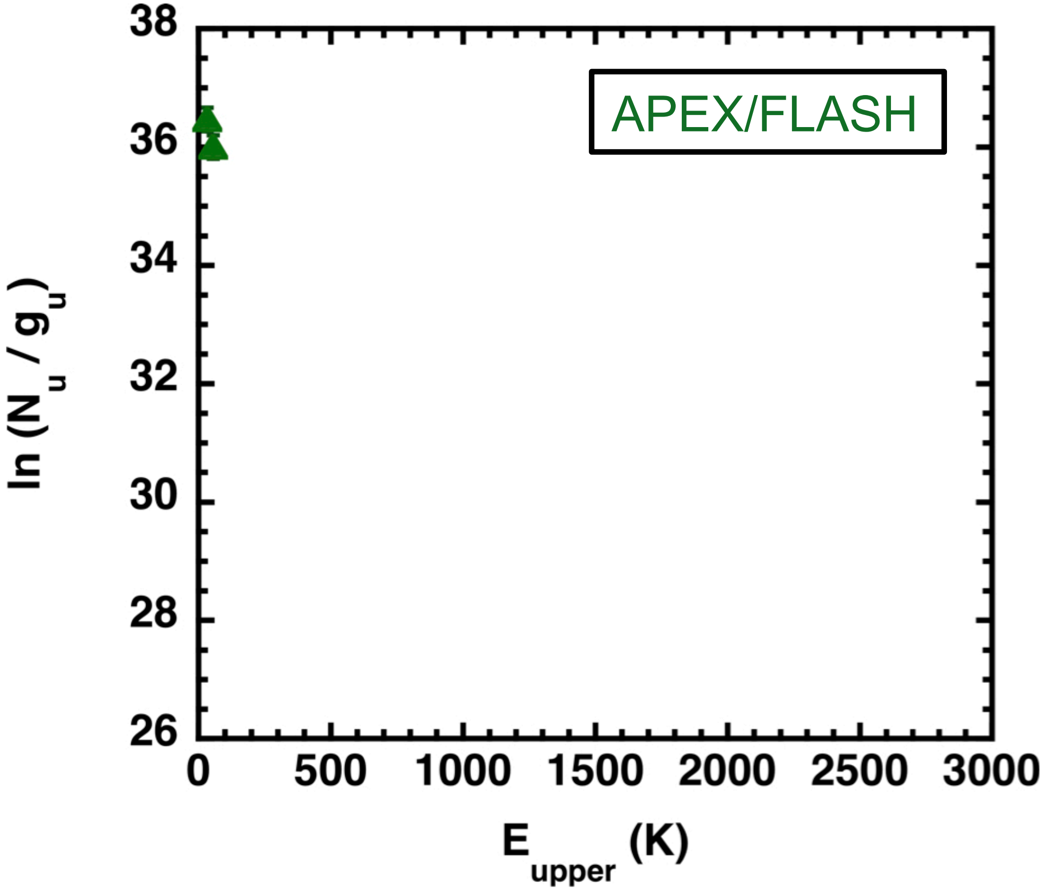

Herschel CO observations

- Summary:
  - APEX => filling factor = 1 for beam of 12.5”, low-*J* are optically thick
  - *Herschel* => higher-*J* lines optically thin, HIFI-PACS cross-calibration
  - Both show a similar gas distribution in the line wings

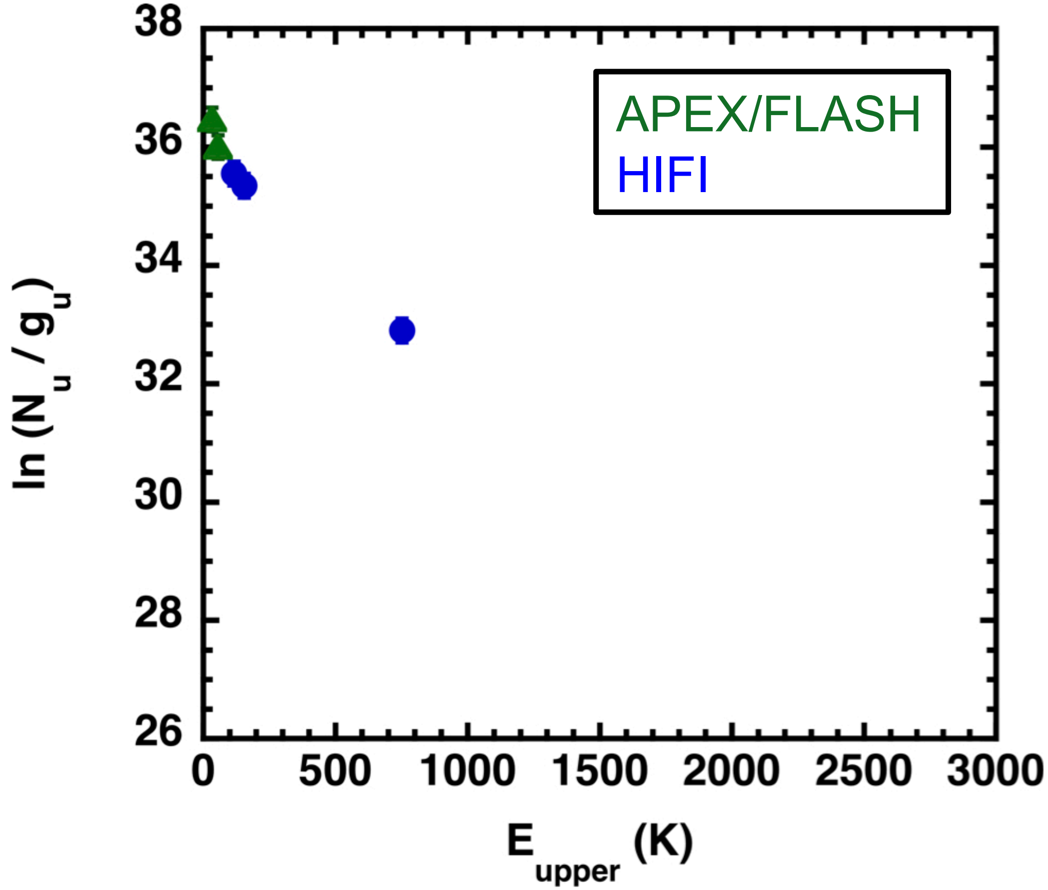

Herschel CO observations

- Summary:
  - APEX => filling factor = 1 for beam of 12.5”, low-*J* are optically thick
  - *Herschel* => higher-*J* lines optically thin, HIFI-PACS cross-calibration
  - Both show a similar gas distribution in the line wings

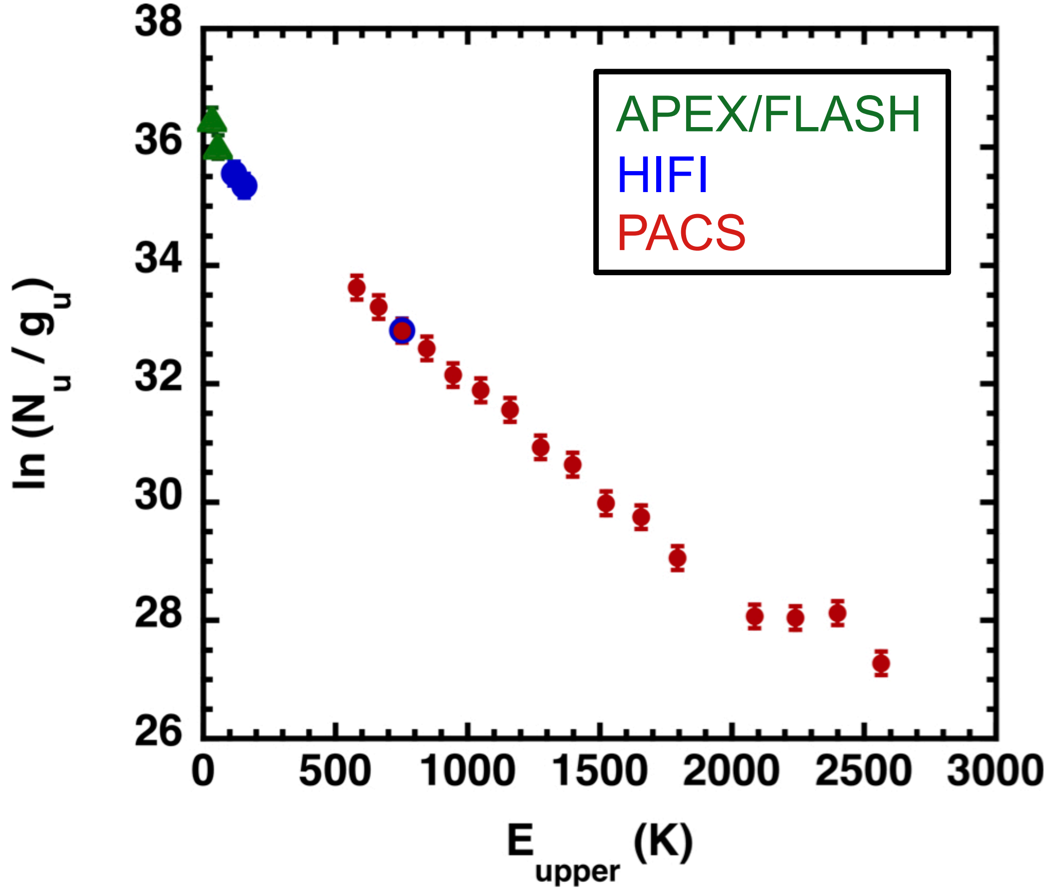

Herschel CO observations

- Summary:
  - APEX => filling factor = 1 for beam of 12.5", low-*J* are optically thick
  - *Herschel* => higher-*J* lines optically thin, HIFI-PACS cross-calibration
  - Both show a similar gas distribution in the line wings

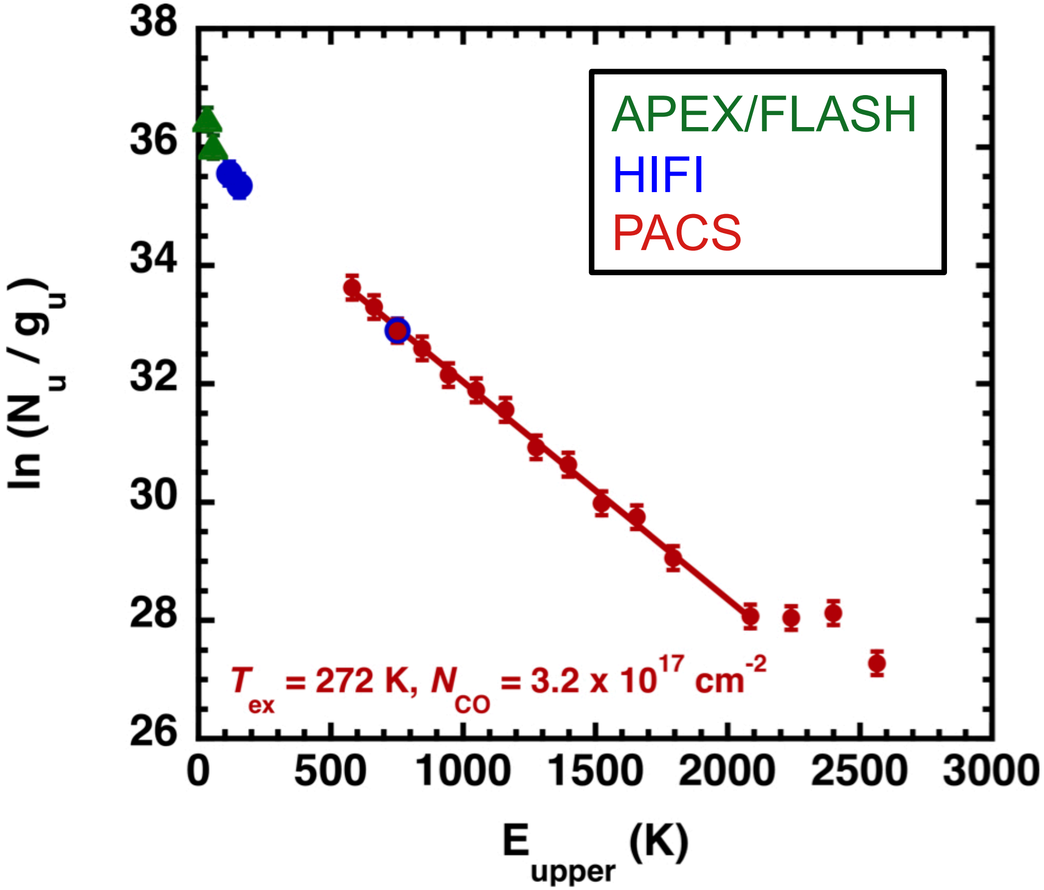

C I & C^+ OBSERVATIONS

APEX CI observations: the data

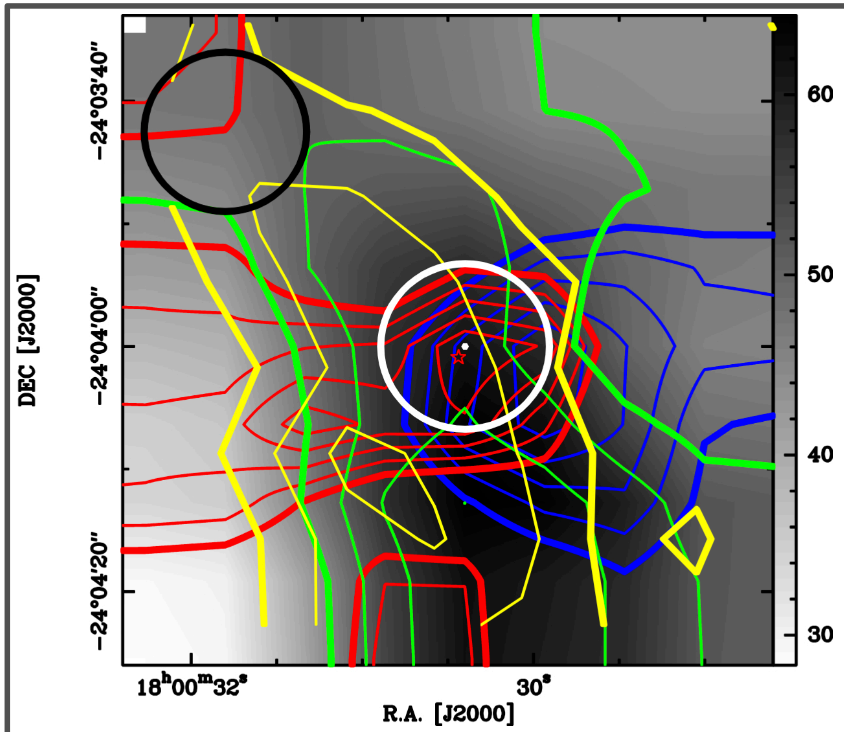

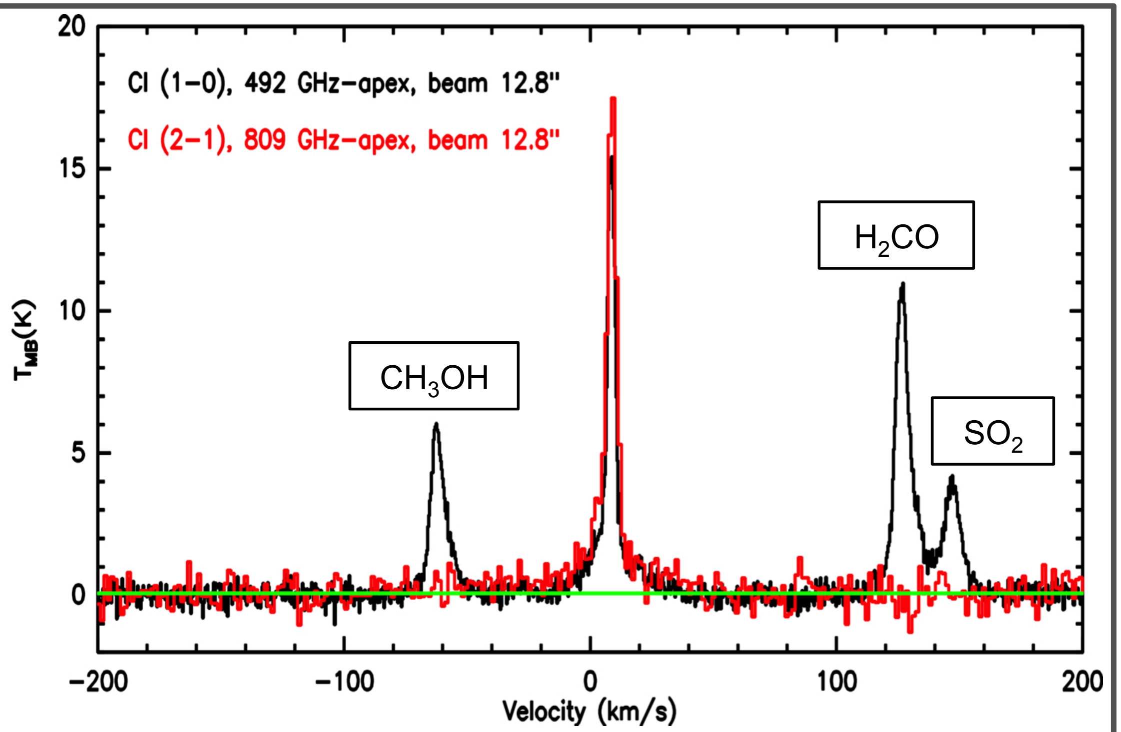

- APEX CI (1-0) line map:
  - total integrated intensity -20 to 40 km/s
  - blue-shifted integrated intensity -20 to 4 km/s
  - red-shifted integrated intensity 20 to 40 km/s
  - ambient CI (1-0) component, 4 to 16.5 km/s
  - ambient CI (2-1) component, 4 to 16.5 km/s

APEX CI observations: an LVG model

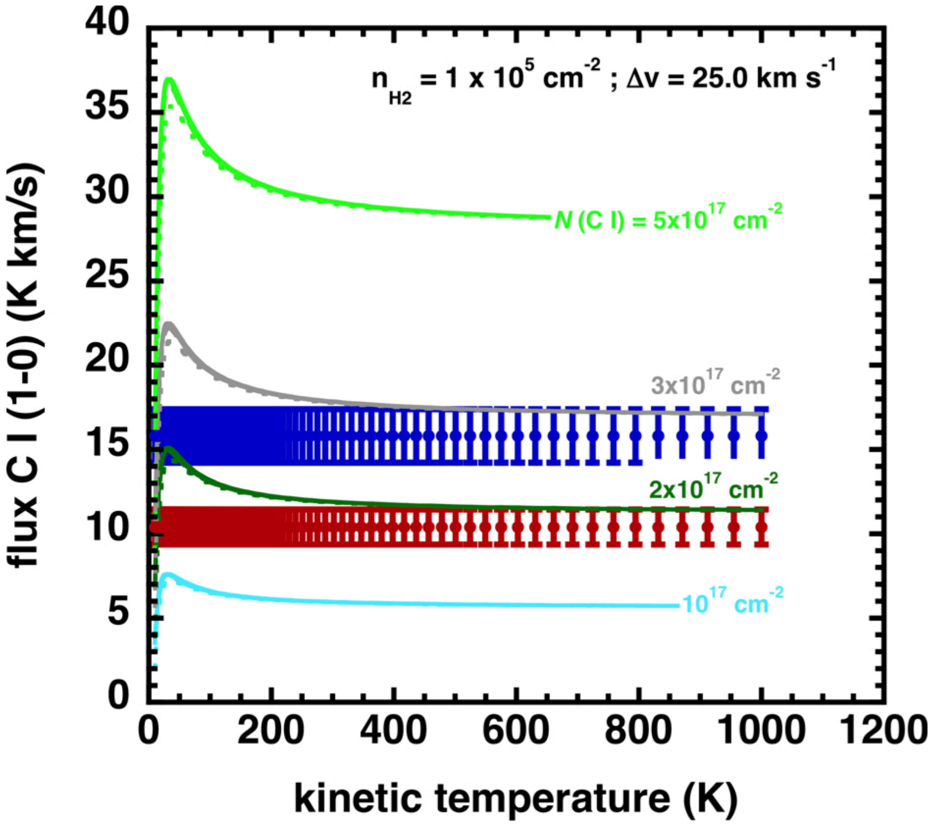

- CI (1-0) integrated intensity: in both blue and red lobes, we seem to find a column density in the range 1-3 x 10^{17} cm^{-2}

APEX CI observations: an LVG model

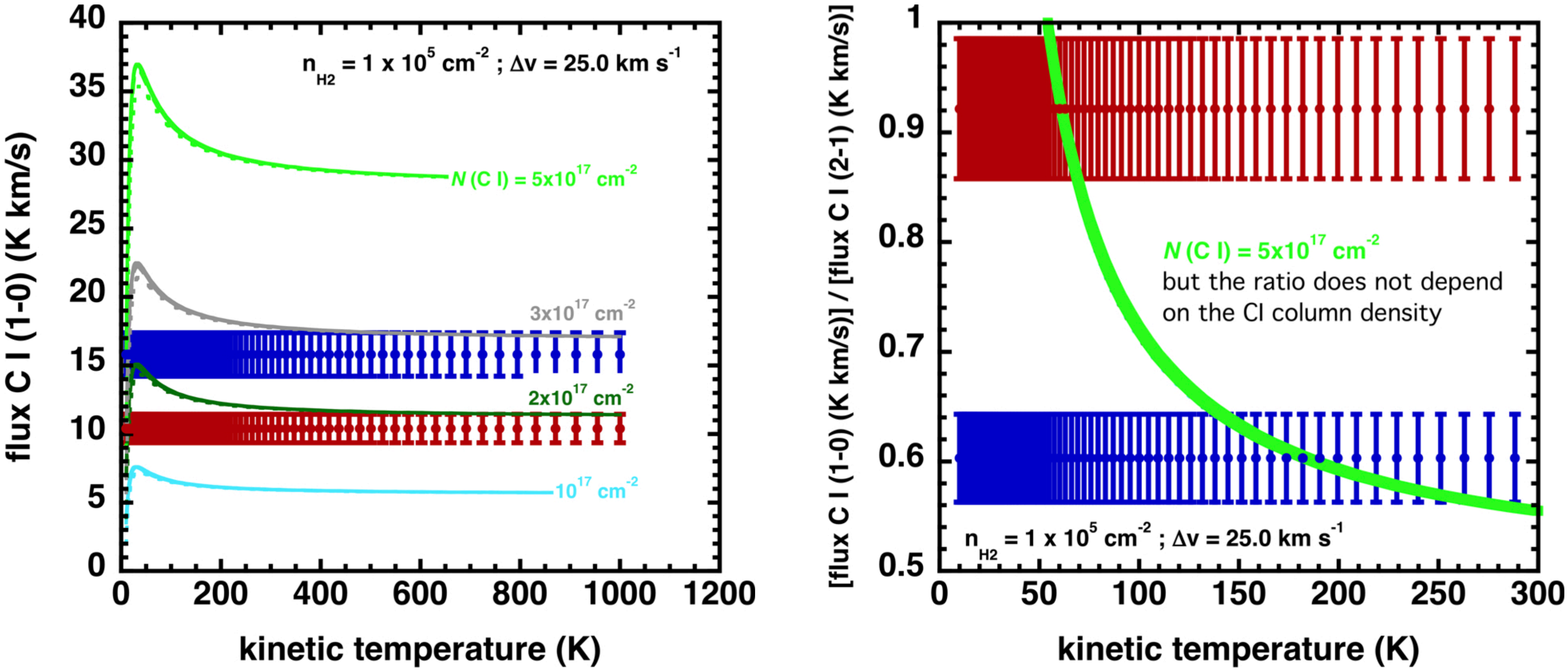

- CI (1-0) integrated intensity: in both blue and red lobes, we seem to find a column density in the range 1-3 x 10^{17} cm^{-2}

- CI (2-1) allows for a determination of the excitation temperature, but this value is subject to higher calibration uncertainties…

Herschel C^+ observations: the data

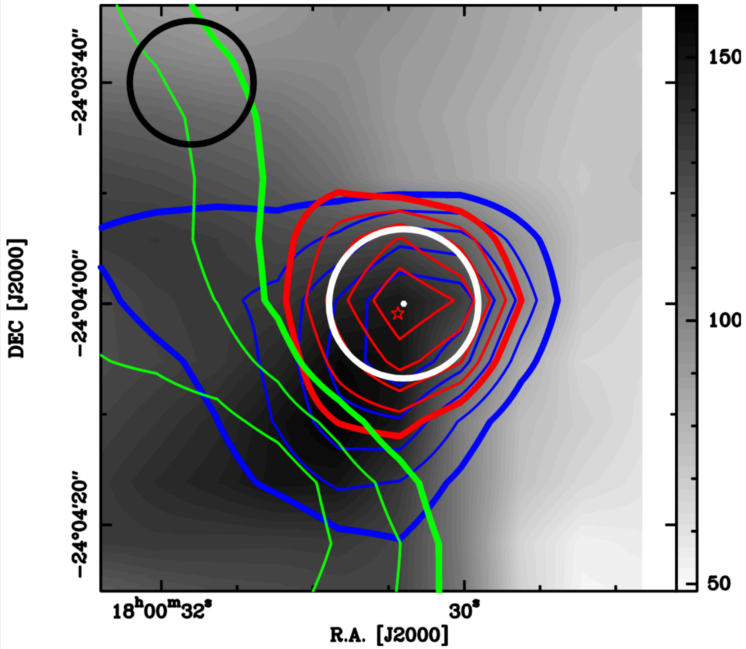

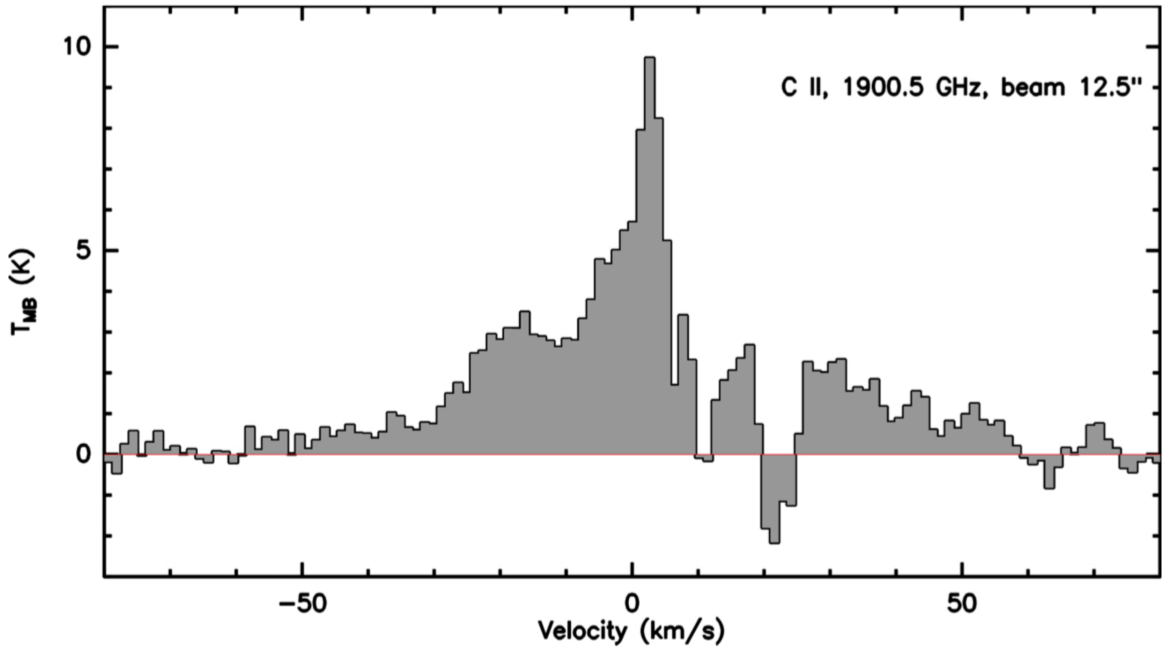

- *Herschel* C^+ line map:
  - total integrated intensity -80 to 80 km/s
  - blue-shifted integrated intensity -80 to 4 km/s
  - red-shifted integrated intensity 25 to 80 km/s
  - ambient integrated intensity 4 to 16.5 km/s

- LTE/optically thin line assumptions: N ~ 3 x 10^{17} cm^{-2} in the blue lobe, N ~ 10^{17} cm^{-2} in the red lobe

PERSPECTIVES

Conclusions

- **Conclusions:**
  - CO over the whole spectral width ~ 3.2 x 10^{17} cm^{-2} with equal distribution in blue, ambient and red component of the spectra
  - C I column density in the range 1-3 x 10^{17} cm^{-2} in each spectral wing
  - C^+ column density of the order of 3 x 10^{17} cm^{-2} in the blue wing, $10^{17} cm^{-2}$ in the red wing

Our modelling strategy

MHD shock code
- 1D stationary (C,J)
- 1D approximated non stationary (CJ)

Inputs: type, b, n_H, $v_{s,}$ (age if CJ)

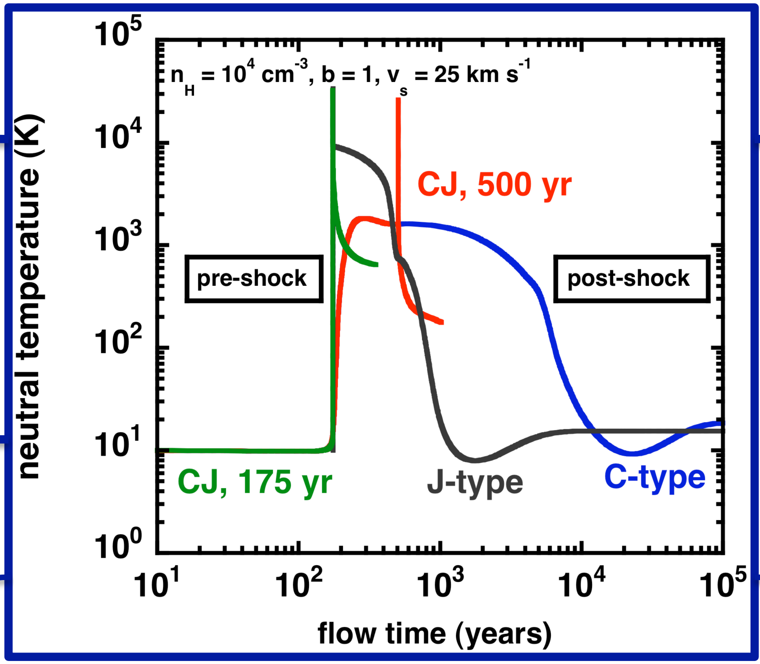

Outputs: physical and chemical structure

Radiation transfer LVG: emissivities, level population at each point of the shock

Constraints on the inputs

macro physics:
Conservation equations
Source terms, ρ, v, T

micro physics:
H_2, chemistry,
grains (physics & chemistry)

Consistent comparisons with the observations
- **(H_2 excitation diagrams)**
- **CO integrated intensity diagrams**

Our modelling strategy

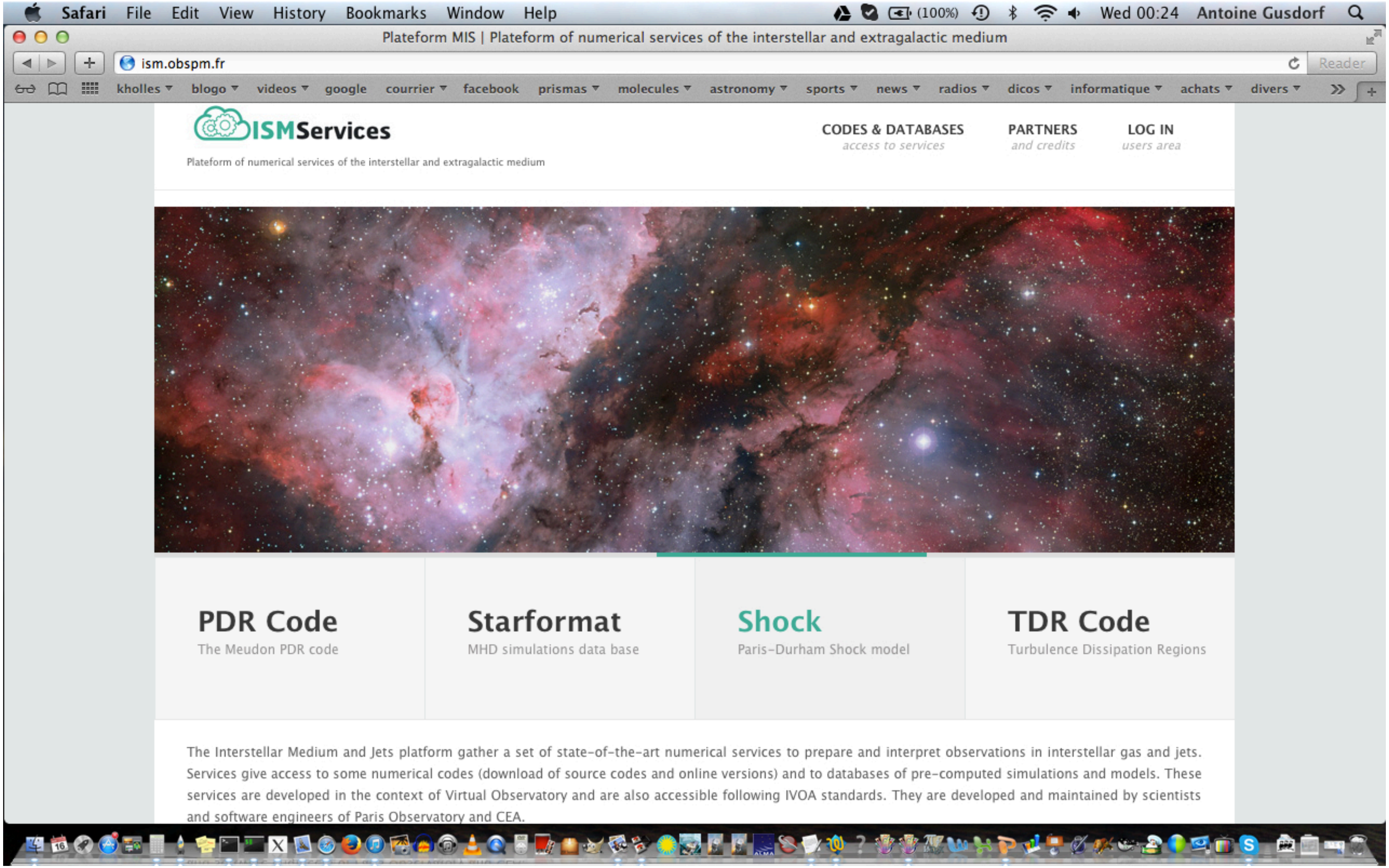

Our modelling strategy